ASIAN JOURNAL OF PHARMACEUTICAL AND CLINICAL RESEARCH

INNOVARE ACADEMIC SCIENCES
Knowledge to Innovation

Vol 18, Issue 10, 2025

Online - 2455-3891
Print - 0974-2441

Research Article

# IDENTIFICATION OF THE ISOLATED COMPONENTS AND STUDY OF ANTIFUNGAL AND ANTICANCER ACTIVITY OF THE EXTRACTS OF *POLYSIPHONIA SUBTILISSIMA* MONTAGNE

**RESHMA CHOUDHURY[1], NITYANANDA SAHOO[2], NIHAR RANJAN KAR[1]***

[1]Department of Pharmacy, School of Pharmacy and Life Sciences, Centurion University of Technology and Management, Odisha, India.
[2]Department of Pharmacy, Nityananda College of Pharmacy, Shergarh, Odisha, India.
*Corresponding author: Nihar Ranjan Kar; Email: nihar_795@rediffmail.com

*Received: 15 June 2025, Revised and Accepted: 28 July 2025*

**ABSTRACT**

**Objective:** We previously identified the presence of different primary and secondary metabolites in *Polysiphonia subtilissima* Montagne, a red alga from the eastern coast of Odisha. Now, we have isolated and identified a few constituents from the bioactive methanol extract and assessed the anticancer and antifungal activities of the three extracts.

**Methods:** Mass spectrometry determined the molecular weights of the components isolated by column chromatography. The probable structures for the m/z values were found from several databanks and validated using Fourier-transform infrared spectroscopy, proton nuclear magnetic resonance, and carbon-13 nuclear magnetic resonance. High-performance liquid chromatography verified component purity. The isolated components were compared to commercial pure compounds. The extracts and their components' 50% inhibitory concentration values were assessed using A549 lung cancer cell line MTT 3-(4,5-Dimethythiazol-2-yl)-2,5-diphenyltetrazolium) tests. The greatest zone of inhibition for antifungal activity was compared to amphotericin B using *Candida albicans*, Microbial Type Culture Collection, and Gene Bank 854.

**Results:** Isolated components A and B, 6-bromoindole and indole-3-acetic acid, had Rf values of 0.94 and 0.86 at 194.97 and 174.06 m/z. Agarose and carrageenan were extracted with structure elucidation. *C. albicans* was inhibited by ethanol extract. The three extracts and isolated components did not inhibit A549 non-small cell lung cancer cell growth.

**Conclusion:** Indole-3-acetic acid (auxin) was extensively observed throughout the winter season due to its association with the growth phase and harvesting period. 6-Bromoindole serves as a precursor for the synthesis of secondary metabolites in algae. Agarose, derived from agar and carrageenan, is ubiquitous in all red algae. The extracts and isolates exhibited no anti-lung cancer efficacy against the A549 cell line. The ethanolic extracts demonstrated notable antifungal efficacy.

**Keywords:** *Polysiphonia subtilissima* Montagne, Indole-3-acetic acid, 6-Bromoindole, agarose, carrageenan, MTT assay, A549, *Candida albicans*, Doxorubicin, Amphotericin B.

 DOI: http://dx.doi.org/10.22159/ajpcr.2025v18i10.55606. Journal homepage: https://innovareacademics.in/journals/index.php/ajpcr

## INTRODUCTION

In the preceding research paper, we examined the chemical composition and biological activities of *Polysiphonia subtilissima* Montagne, a marine red alga collected from the eastern coast of Odisha [1]. Qualitative analysis of the extracts confirmed the presence of various primary and secondary metabolites. The extracts were evaluated for their antioxidant, anti-inflammatory, antibacterial, and anticoagulant properties, alongside the quantification of agar, carrageenan, total fatty acids, total flavonoids, and total phenolics. The methanolic extract at 515.5 nm exhibited the highest concentrations of total phenolics (3.14 mg), flavonoids (2.72 mg), and fatty acids (0.12 mg in ethyl acetate and 0.1 mg in chloroform). The antioxidant activity was found to be 95% in the methanolic extract. The aqueous extract exhibited the highest anti-inflammatory activity, measuring 72.13% and 89.61% at concentrations of 100 and 200 µg/mL, respectively. The ethanolic fraction exhibited maximum bactericidal inhibitions of 77.6%, 58%, and 73.7% at a concentration of 500 µg/mL. The water extract demonstrated anticoagulant activity, with an activated partial thromboplastin time of 139 s, prothrombin time of 70 s, and thrombin time of 60 s. Thus, the aqueous, methanolic, and ethanolic extracts were of prime importance for the isolation and characterization of the algal chemical composition. To perform the isolation of the components, a sequential solvent extraction was carried out based on their polarity. The methanolic extract showed two spots with excellent resolution. Preparative thin-layer chromatography (TLC) plates and column chromatography were used for quantitative separation. A high-performance liquid chromatography (HPLC) analysis of the separated components confirmed their purity. The isolated compounds were subjected to mass spectral (MS) analysis utilizing negative electrospray ionization mass spectrometry (ESI-MS) mode at low energy to determine their molecular weight and analyze their structure. Multiple databases were queried to determine the likely structure of each identified molecular weight. These databases included NIST Chemistry Webbook SRD 69 [2], Natural Products Atlas [3], Natural Product Activity and Species Source Database [4], NIST/EPA/NIH MS Library [5], Wiley Registry of MS Data, Spectral Database for Organic Compounds (SDBS) [6], Global Natural Products Social (GNPS) Molecular Networking [7], as well as chemical databases such as PubChem [8], ChemSpider [9], ChEMBL [10], and ZINC 20 Database [11]. We also consulted databases specific to seaweed metabolites, namely, AlgaeBase [12] and the Comprehensive Marine Natural Products Database [13]. Following the determination of the likely structures, the proton nuclear magnetic resonance ($^{1}$HNMR), carbon-13 nuclear magnetic resonance ($^{13}$C NMR), and infrared (IR) spectra were obtained for each individual component. Subsequently, the highly pure standard compounds were acquired, and the spectral analysis of the pure standards was conducted and compared with the isolated components. Agar and carrageenan were separated using standard protocols and thereafter subjected to spectral analysis. A literature survey reveals that red seaweed extracts generally exhibit anticancer activity against various cancer types, including breast,

colon, lung, and others [14-16]. Presently, one lung cancer strain, that is, A549, has been selected for biological evaluation. The A549 is a human non-small cell lung cancer (NSCLC) cell line [17]. Using the MTT assay method [18], we studied the three extracts along with the two isolates for anticancer activity on A549 (cells isolated from the lung carcinomatous tissue of a 58-year-old Caucasian male patient) and antifungal activity on a fungal culture *Candida albicans*, using the zone inhibition method [19]. Doxorubicin was applied as a standard in anticancer activity studies [20], while amphotericin B was used in antifungal activity studies [21].

## METHODS

All chemical reagents, standard compounds, and solvents used in the studies were purchased from Himedia (India), Merck (India), SRL Pvt. Ltd., and Loba Chemie (India), unless otherwise noted, and were utilized without further purification. Merck (India) supplied the pre-coated plates of TLC aluminum sheets (sheet L × W 5 cm × 7.5 cm), silica gel 60 $F_{254}$. All ultraviolet (UV)-visible spectroscopic measurements were made using the UV-2450, made by Shimadzu in Japan. The fungal culture (*C. albicans*, MTCC 854) was obtained from the Microbial Type Culture Collection and Gene Bank (MTCC), Chandigarh, India, whereas the A549 cell line was acquired from NCCS Pune, India. Uncorrected melting points were measured in open capillary tubes. FT/IR-4100 type A model manufactured by Bruker was used to record the Fourier-transform infrared spectroscopy (FTIR) spectral signals.JNM-ECZ500R/S1 spectrometer by JEOL 500 and 400 MHz spectrometers were used to record the $^{1}$HNMR and $^{13}$C NMR spectra (500 MHz, 400 MHz, and 125 MHz for $^{1}$HNMR and $^{13}$C NMR, respectively). The Shimadzu LC-MS, LC-2010EVwith Shimadzu Prominence HPLC System, was used for MS analysis with ESI probes mass spectrometers. Dionex 1996-2006 Version 6.80 SR15 Build 4656 (243203) was used for the HPLC investigation, along with a UV detector and Chromeleon (c) software. Bond Elut C18 and HLB solid phase extraction (SPE) cartridges (Agilent) were used for in-process purification.1188/1 Rotary Vacuum Flash Evaporator (Buchhi Type) by JSGW was used for distillation. The microprocessor-based Systonic tabletop pH-mV temperature meter S-906 was used for pH measurement. JSI UV Inspection Cabinet Double Tubes 144 was used to locate the spots in TLC plates. It is crucial to carryout pre-treatment, which entails cleaning, washing, and drying the crude red algae samples, before beginning any extraction.

### Isolation and purification of the extracts

Subsequent to the detection of higher biological activities in the methanol extract, 20g of the red algae samples were re-extracted and mixed with methanol and a 5% aqueous Hydrochloride (HCl) solution for the extraction of alkaloids. The methanol extract was acidified by the addition of 10% acetic acid to attain a pH range of 2.5–3.0, thereafter dissolving it in water. The content was partitioned into two fractions. To the first aqueous fraction, 100 mL of ethyl acetate was added and extracted thrice. The ethyl acetate fractions were combined and concentrated at 50°C with a rotary evaporator. The residue was solubilized in 50 ml of methanol. Bond Elut C18 and HLB SPE cartridges (Agilent) were subsequently employed to enhance the in-process purification of the extract. The second part of the divided fraction underwent extraction with dichloromethane, followed by alkalization with 25% ammonia to achieve a pH of 8.5. It was subsequently extracted with dichloromethane to obtain any alkaloids or basic components [22,23].

Due to the enhanced possibility of obtaining halogenated indole derivatives from the crude sample, 20 g of the dry powdered sample was submerged in 200 mL of methanol and agitated for 24 h at ambient temperature. The product was subsequently filtered, and the filtrate was evaporated at 50°C. The procedure was repeated thrice by consolidating the methanol layers each time to obtain a substantial yield of the components. The crude extract was solubilized in water and partitioned with ethyl acetate three times. The organic layer was collected and dried under anhydrous sodium sulfate and subsequently evaporated at 50°C. Silica gel column chromatography was employed for purification, utilizing a gradient of hexane and ethyl acetate, commencing with 100% hexane and progressively increasing the concentration of ethyl acetate. The fractions were collected with an interval of one minute. The TLC of the fraction exhibits fluorescence under UV light, facilitating monitoring during purification. The fractions were analyzed via TLC and seen under ultraviolet light at 254 nm. We used preparative TLC to get the components as separate compounds. Preparative TLC glass plates of size L × W; 20 cm × 20 cm, with PLC silica gel 60 F254, were used to coat the plates. The adsorbent layer thicknesses were kept >100 μm. HPLC studies of the two components were carried out in good resolution and were benchmarked with commercially available standard compounds [24].

### Identification and structural elucidation of the two isolated components

The two isolated components were tested for the determination of molecular weights in negative ion mode ESI-MS. After careful determination of the molecular weight, the repository NIST Chemistry Webbook, SRD 69, NIST Chemistry WebBook-SRD 69, National Institute of Standards and Technology, was searched for probable organic compounds with that molecular weight. After qualitative analysis, it was revealed that the two components are not alkaloids, and we searched various natural compound databases, including the Natural Products Atlas, Natural Product Activity and Species Source Database, spectral libraries like the NIST/EPA/NIH MS Library, Wiley Registry of MS Data, SDBS, GNPS Molecular Networking, and some chemical databases such as PubChem, ChemSpider, ChEMBL, and ZINC Database. Seaweed metabolite databases, AlgaeBase, and the Comprehensive

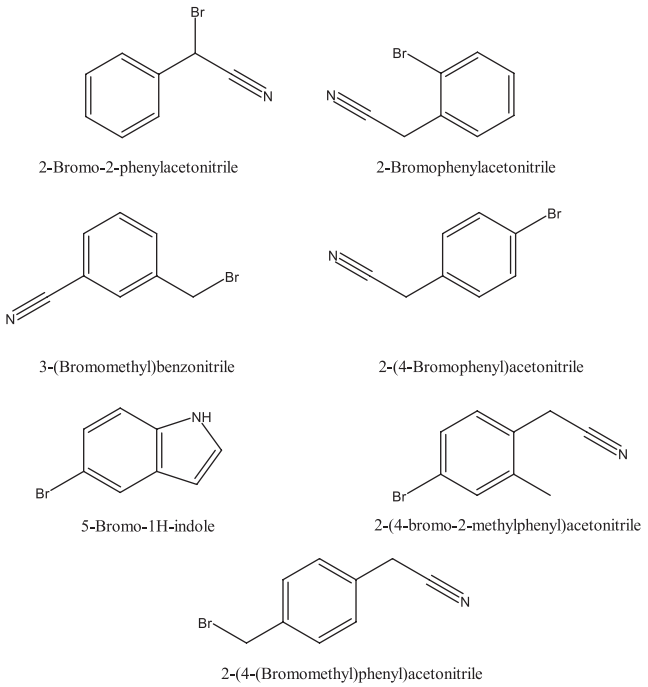


**Fig. 1: Seven possible structures with molecular weight of 193.97 extracted from the database**

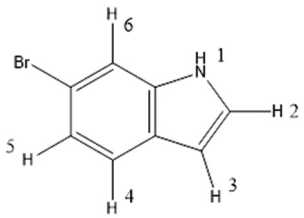

**Fig. 2: Number representation of hydrogens of component A**

Marine Natural Products Database were also referred to. The IR spectra, $^{1}$HNMR, $^{13}$C NMR, and elemental analysis of the two components were done along with the standard compounds commercially purchased in high purity to compare the spectral data to confirm their structure.

**Extraction of agar from *P. subtilissima* Montage**

The extraction of agar from pre-treated *P. subtilissima* Montagewas carried out using combined ultrasound-assisted hot water extraction mechanisms, as outlined by Martinez-Sanz *et al.* [25]. Here, 50 g of desiccated seaweed powder were submerged in 500 mL of purified water and subjected to a temperature of 90°C for a duration of 2 h. Following temperature stabilization, the ultrasound probe IP-400 (Hielscher GmbH, Germany) was submerged and subjected to a sonication treatment with a maximum power of 400W and a consistent frequency of 24 kHz for a duration of 30 min. Subsequently, the agar-based solution was separated from the solid residue by filtration against muslin cloth. Following gelation, the filtrate was frozen overnight at −21°C. Subsequently, the material underwent two freeze-thaw cycles at temperatures of −21°C and 25°C to enhance the strength characteristics of the gels. The resulting gel was then dried by a freeze dryer Lyophilizer (ANM Freeze Dryer 4 Layers FD-50) and qualitatively tested for the presence of agar [1].

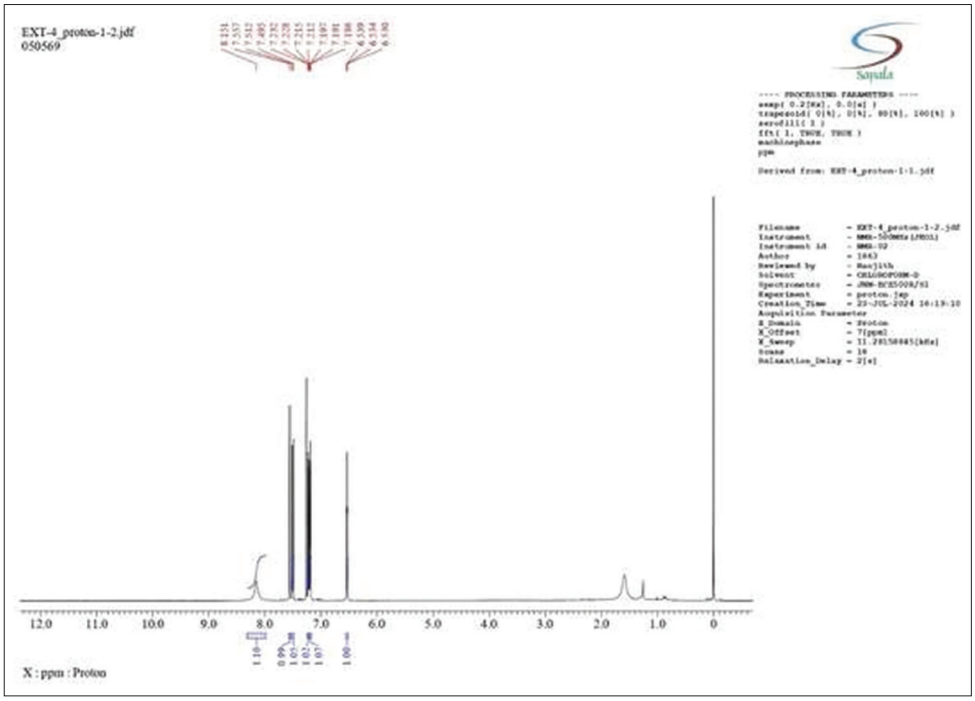


**Fig. 3: Proton nuclear magnetic resonance spectra of component A**

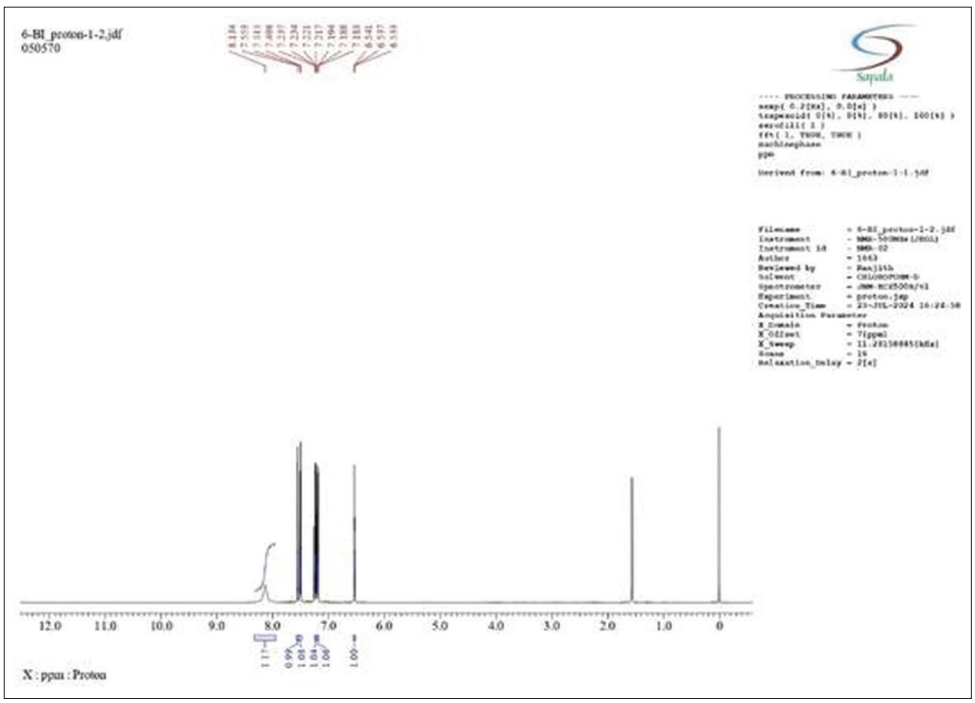


**Fig. 4: Proton nuclear magnetic resonance spectra of standard 6-bromoindole (Sigma Aldrich)**

**Recovery of purified agarose from the extracted agar**

We adopted this method from the US patent of Province and Camden [26]. At room temperature, a 50 mL ethylene glycol solution was mixed with 5 g of extracted agar. To ensure that the agar was completely dissolved, the solution was heated to 105°C and maintained there for an hour.

A fine precipitate formed when the agar-containing solution was cooled after being taken off of the heat source. Overnight, the slurry was placed in a freezer set at −20°C, which caused more precipitate to form. Fifty milliliters of cooled isopropyl alcohol at −20°C were added to the slurry. After 2 h of stirring, the mixture was put back in the freezer overnight. The slurry was centrifuged (EURO-ELECTRA-BL laboratory centrifuge) after being agitated to reconstitute it the following day. After two additional isopropyl alcohol washes, the centrifuge cake was dried in a hot air oven that was set to 55°C. The result was a fine, free-flowing white powder made from agarose. The agarose product had a 23% recovery yield. IR, $^{1}$HNMR, $^{13}$C NMR, and elemental analysis tests were performed on the extracted components.

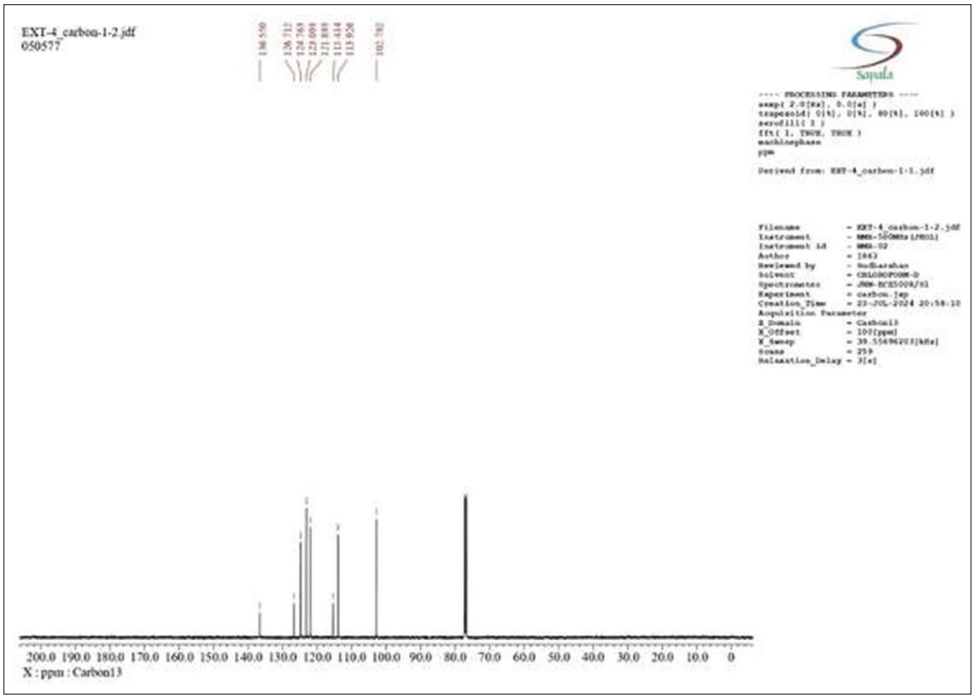


**Fig. 5: Carbon-13 nuclear magnetic resonance spectra of component A**

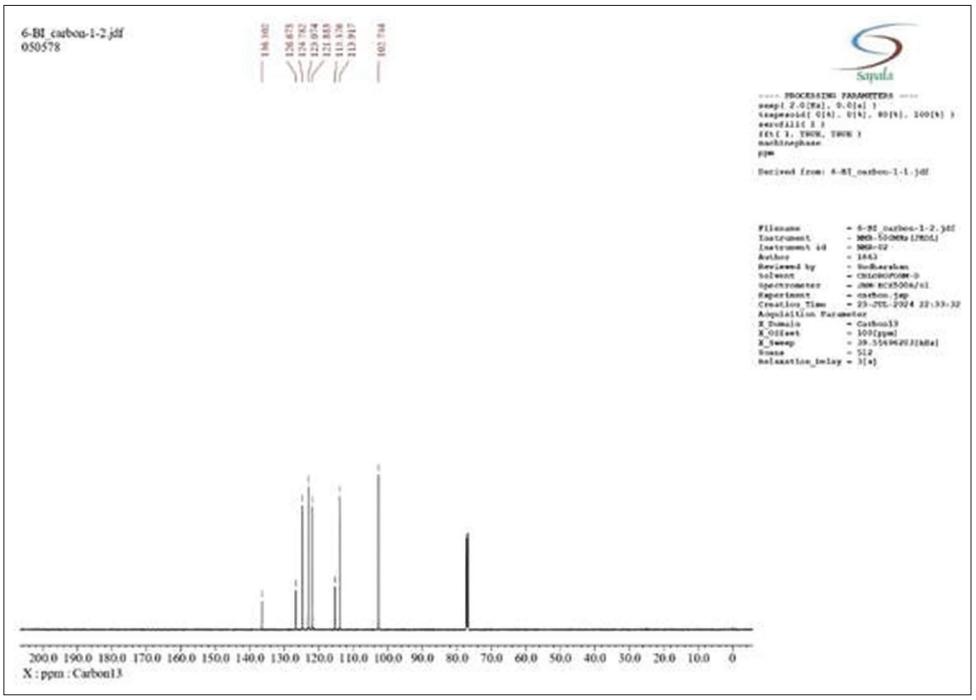


**Fig. 6: Carbon-13 nuclear magnetic resonance spectra of standard 6-bromoindole (Sigma Aldrich)**

**Extraction of Carrageenan from *P. subtilissima* Montage by alkaline treatment method [27,28]**

Samples weighing 10 g were pre-treated by immersing in 0.05 M potassium hydroxide and heated to a temperature range of 70–90°C for a duration of 3 h. This treatment enhances gel strength and eliminates contaminants. Treated samples were immersed in 200 mL of distilled water and heated to 80–90°C for 4 h with periodic stirring. The carrageenan dissolves in water, creating a viscous solution. The hot extract was filtered through a fine muslin cloth to isolate the solid remains (cell debris). To precipitate the carrageenan, the filtrate was chilled, and isopropanol was added in a 1:2 ratio to the water extract. The precipitated carrageenan was harvested and dehydrated at 50–60°C in a drying oven. Upon complete desiccation, it was pulverized into a fine powder.

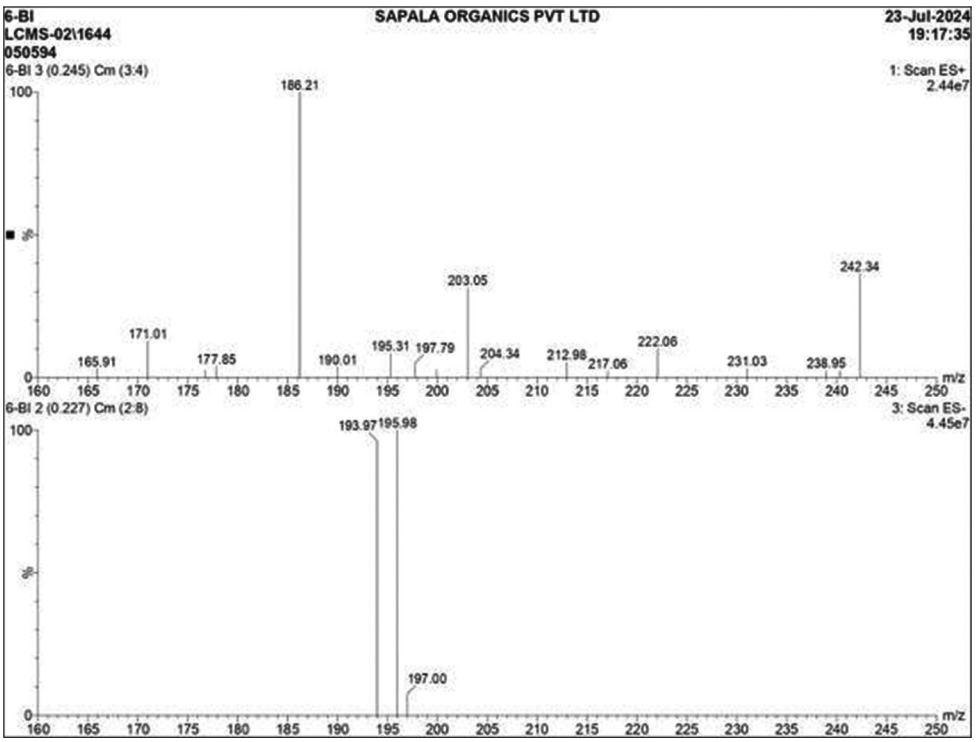


**Fig. 7: Mass spectra of component A**

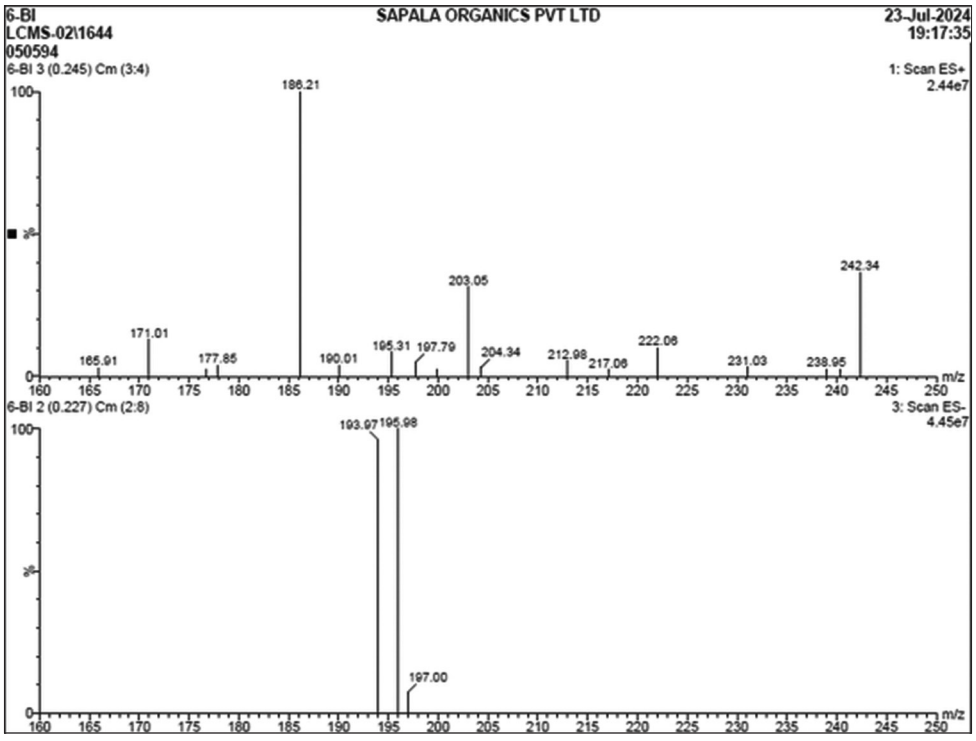


**Fig. 8: Mass spectra of standard 6-bromoindole (Sigma Aldrich)**

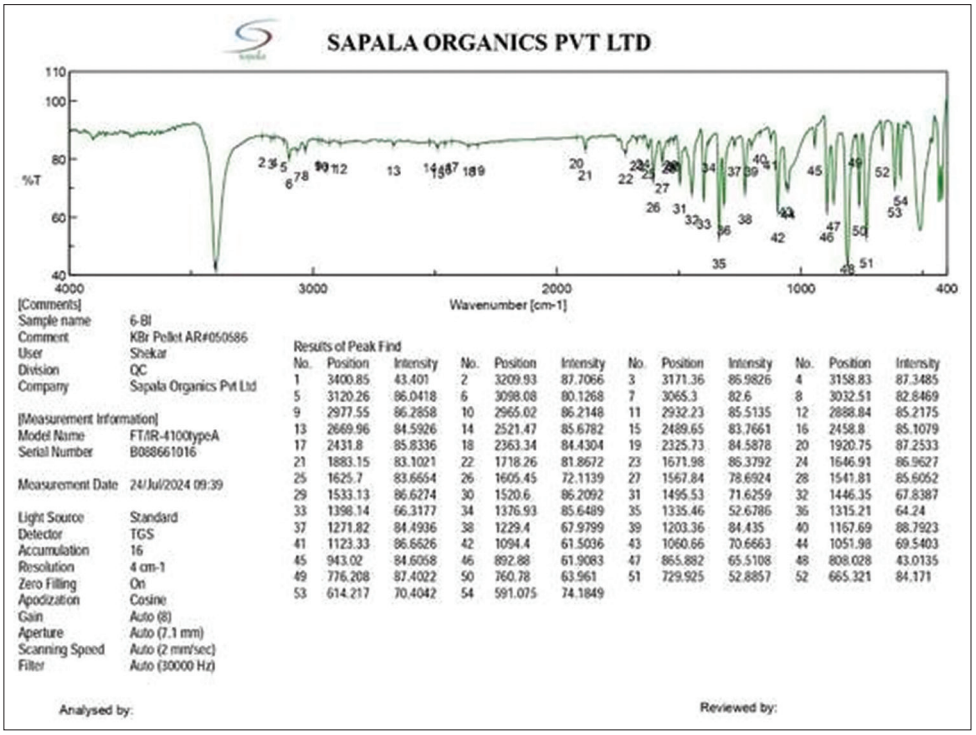


**Fig. 9: Fourier-transform infrared spectroscopy spectra of component A**

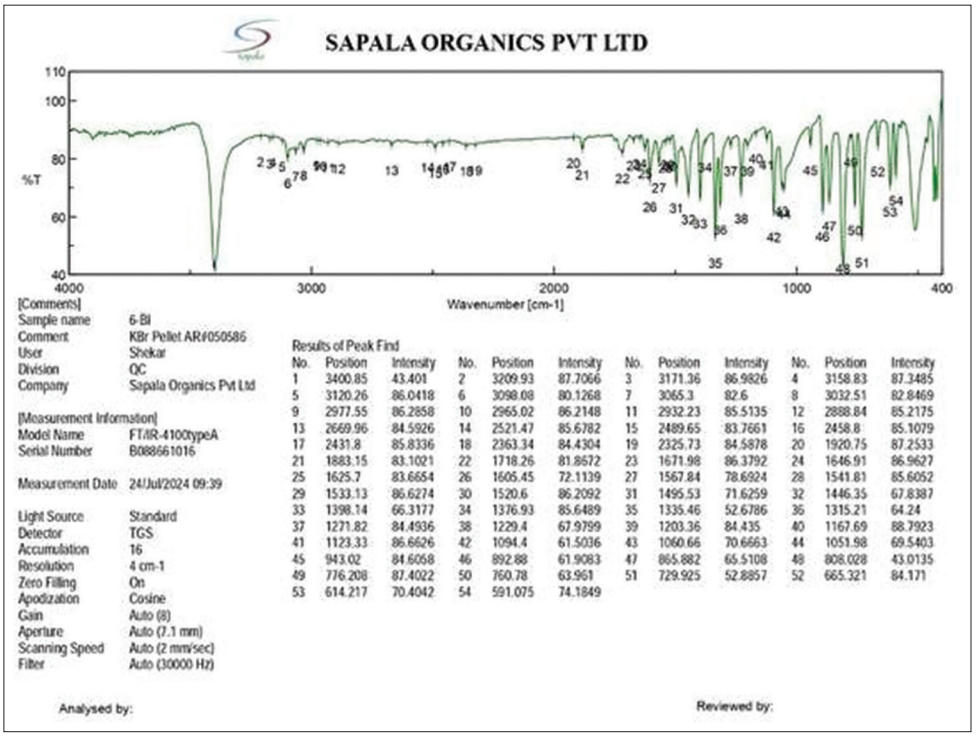


**Fig. 10: Fourier-transform infrared spectroscopy spectra of standard 6-bromoindole**

***In vitro* cytotoxicity evaluation of the extracts on A549 by MTT assay [29,30]**

The cytotoxic potential of the three extracts and the two isolates on the A549 cell line was assessed using the MTT test. 10% FBS (fetal bovine serum-HIMEDIA-RM 10432) and 1% antibiotic solution (Penicillin-Streptomycin-Sigma-Aldrich P0781) were added to DMEM media (Dulbecco's Modified Eagle media-AT149-1L-HIMEDIA) in a 96-well plate, and the cells (10,000 cells/well) were cultivated for 24 h at 37°C with 5% $CO_2$. Different concentrations of the samples (1, 10, 50, 100, 250, 500, and 1000 µg/mL) were applied to the cells the next day. To get varying quantities in incomplete cell culture medium (without FBS), a stock solution of samples was made and further diluted. Following a 24 h incubation period, the cell culture was supplemented with MTT solution (5 mg/mL) and incubated for an additional 2 h. Cells without MTT were referred to as blanks, while cells without treatment were referred to as controls. Following the test, the culture supernatant

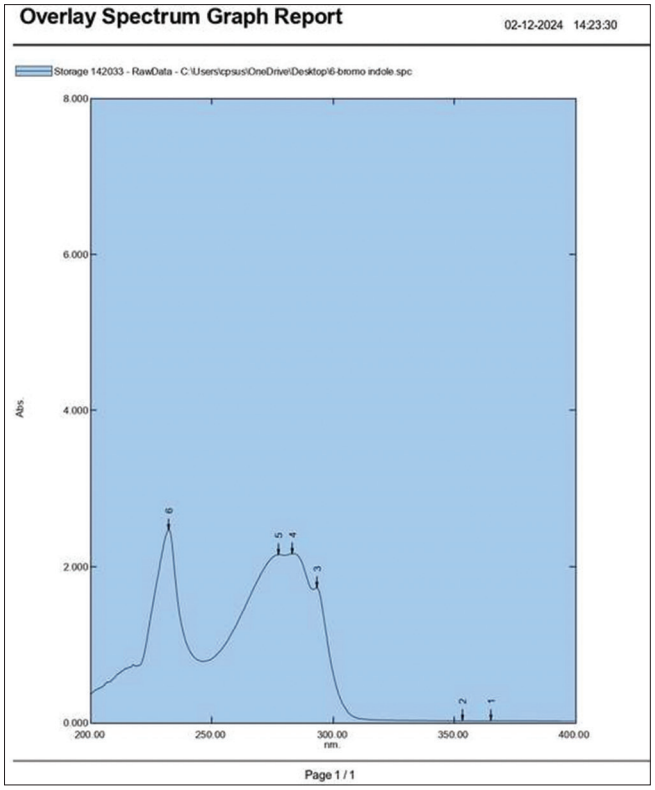


**Fig. 11: Ultraviolet spectrum of standard 6-bromoindole**

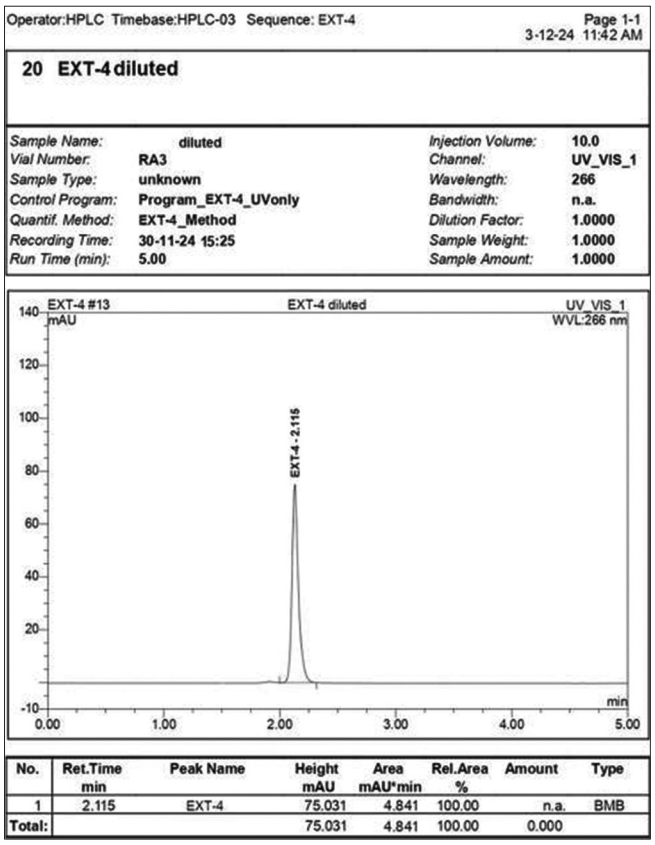


| No. | Ret.Time min | Peak Name | Height mAU | Area mAU*min | Rel.Area % | Amount | Type |
|---|---|---|---|---|---|---|---|
| 1 | 2.115 | EXT-4 | 75.031 | 4.841 | 100.00 | n.a. | BMB |
| Total: | | | 75.031 | 4.841 | 100.00 | 0.000 | |

**Fig. 12: High-performance liquid chromatography peak of component A with Rt 2.115**

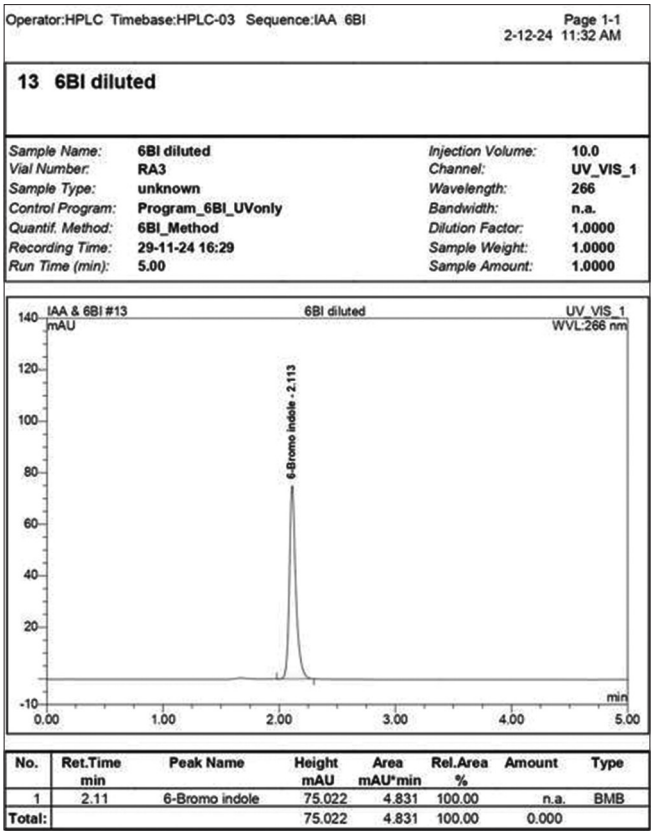


| No. | Ret.Time min | Peak Name | Height mAU | Area mAU*min | Rel.Area % | Amount | Type |
|---|---|---|---|---|---|---|---|
| 1 | 2.11 | 6-Bromo indole | 75.022 | 4.831 | 100.00 | n.a. | BMB |
| Total: | | | 75.022 | 4.831 | 100.00 | 0.000 | |

**Fig. 13: High-performance liquid chromatography peak of standard 6-bromoindole with Rt 2.113**

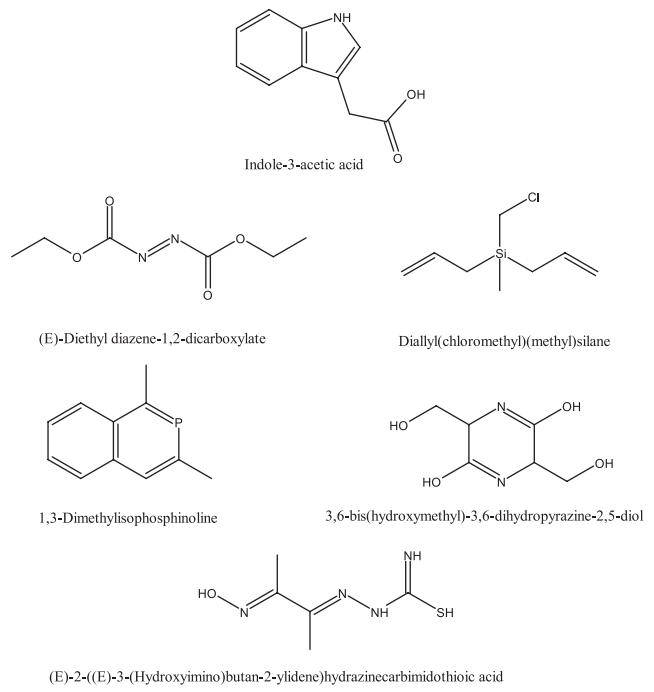


**Fig. 14: Six possible structures with molecular weight of 174.06 extracted from the database**

was removed, and the cell layer matrix was dissolved using 100 µl of dimethyl sulfoxide (DMSO–SRL–Cat no.–67685). An enzyme-linked immunosorbent assay plate reader (iMark, Biorad, USA) was then used to read this at 540 nm. GraphPad Prism-6 was used to determine the 50% inhibitory concentration ($IC_{50}$). Three test replicates were performed, and the mean±standard deviation (SD) was calculated to

display the $IC_{50}$. Non-linear regression (4-parameter logistic model/hill equation) was used to determine the $IC_{50}$ values.

% Viable cells=(Atest/AControl) * 100 (Atest=Absorbance of test sample) (AControl=Absorbance of Control)

**Assay of anti-fungal activity of the isolates and extracts by zone inhibition method [31,32]**

The zone inhibition method (also known as the Kirby-Bauer method) was used to evaluate the antifungal activity. The fungal culture, *C. albicans*, prepared at a 0.5 McFarland Unit, or roughly $1.5 \times 10^8$ CFU/mL from Sabouraud dextrose broth, was spread out in 100 µL to inoculate the Sabouraud dextrose agar plates. Discs containing 10 µL of different concentrations (10 µL to 20 mg/mL of the five samples) were then placed. An Amphotericin B disc (50 µg) was used as the positive control, and one disc on each plate was filled entirely with solvent, acting as the vehicle control. An incubator (Basil Scientific Corp. India) was used to incubate the *Candida albicans* plates for 24 hours at 37 °C. To determine the maximum zone of inhibition (MZOI), the diameter of the clear area around the test substance was measured with a caliper. The defined areas around the disc were measured and documented. Three test replicates were performed, and the mean±SD was calculated to display the MOZI.

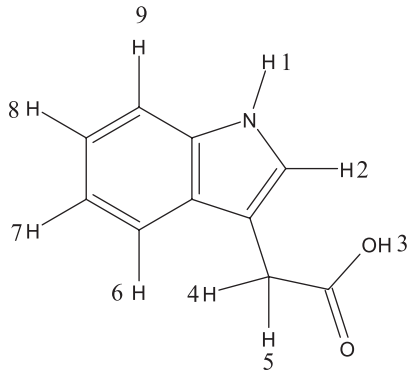


**Fig. 15: Number representation of hydrogens of component B**

## RESULTS AND DISCUSSION

**Extraction and isolation**

Halogenated indole (component A), Indole-3-acetic acid (component B), agarose (component C), and carrageenan (component D) were extracted and isolated in pure form. The resolution of the spots of component A and B was finally observed in water: methanol in 7:3. The spots were recorded in a UV chamber and in an iodine chamber. The ethanolic extract was spotted on TLC, and different solvent systems were used to resolve the components.

**Characterization of the isolated components using spectroscopic analysis**

In every case, after characterization of the isolated component, each one was benchmarked by comparing the data obtained from highly pure standards from Sigma Aldrich. The isolated components were tested individually for MS analysis, $^1$HNMR, $^{13}$C NMR, and FTIR.

**Structural characterization of component A**

The component **A**, with an $R_f$ value of 0.94, exhibited two peaks at 193.97 (M+) and 195.98 (M+1) (Fig. 8), demonstrating an intensity ratio of around 49:51, almost equal height (Fig. 7). This is a distinctive peak for compounds that contain one bromine atom in the molecule. Different databases were searched for the probable compound with a molecular weight of approximately 193.97, and we found seven possible structures, namely, 2-Bromo-2-phenylacetonitrile, 2-Bromophenylacetonitrile, 3-Bromomethylbenzonitrile, 2-Bromophenylacetonitrile, 5-Bromo-1H-indole, 2-Bromo-2-methylphenylacetonitrile, and 2-Bromo-4-phenylacetonitrile, which are depicted in (Fig. 1).

The $^1$HNMR and $^{13}$C NMR spectra of all the probable structures were predicted using Mestre Nova [33]. Spectral data for component A were collected and matched with the probable compounds. The $^1$HNMR data show that the component A might be 6-Bromo-1H-indole, which is a positional isomer of one of the probable structures, that is, 5-Bromo-1H-indole. The interpretation of the spectral data is given below.

*Component A*

Melting point of component A (6-Bromoindole), (Fig:2) was found to be 92-94°C.

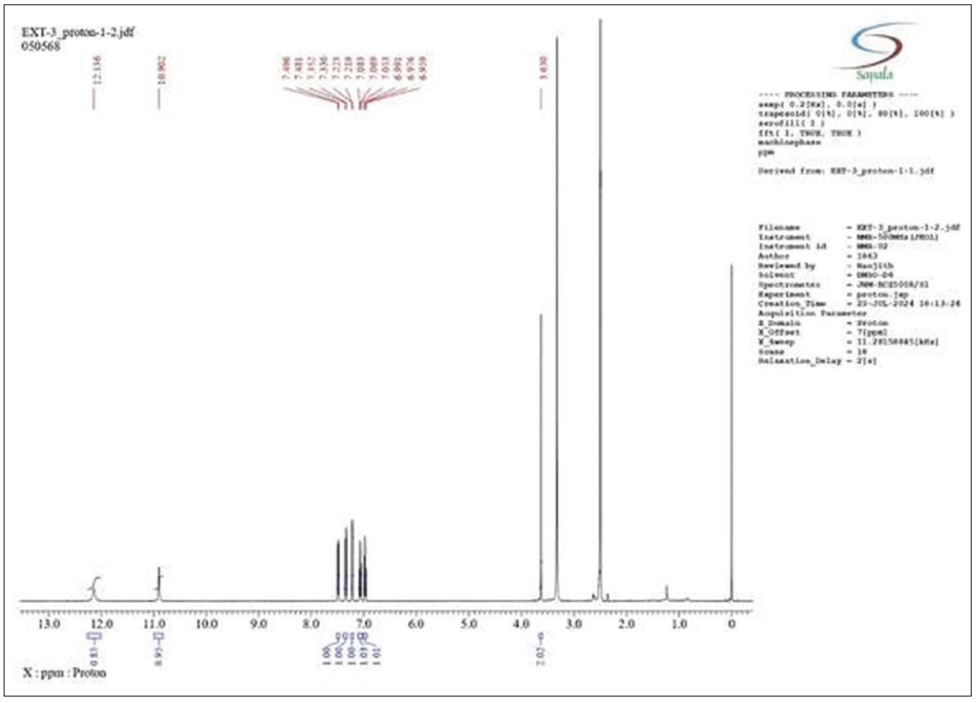


**Fig.16: Proton nuclear magnetic resonance spectrum of component B**

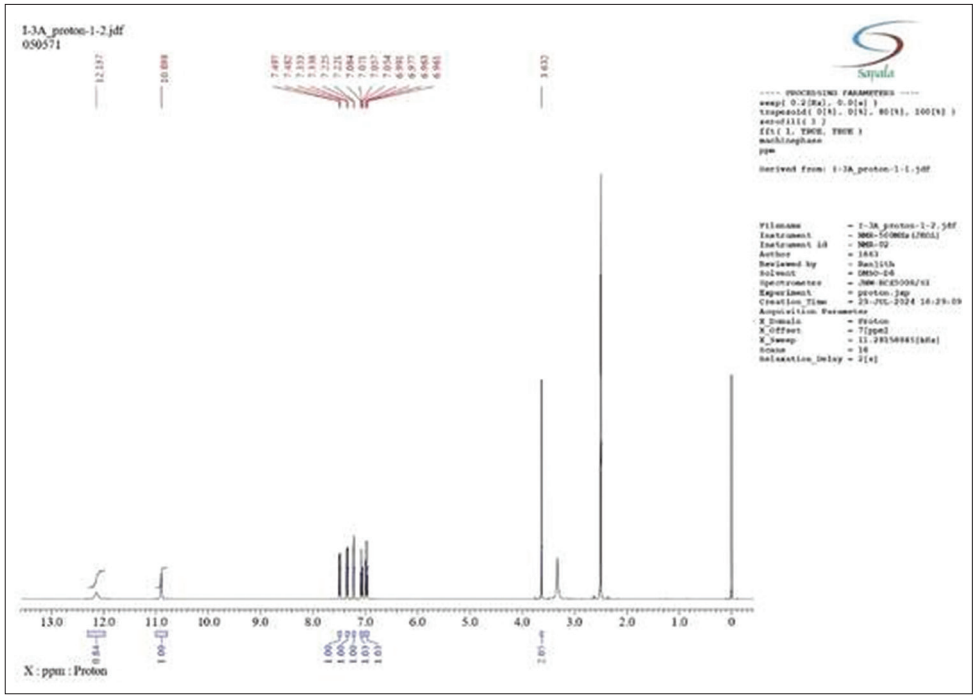


**Fig. 17: Proton nuclear magnetic resonance spectrum of standard indole-3-acetic acid**

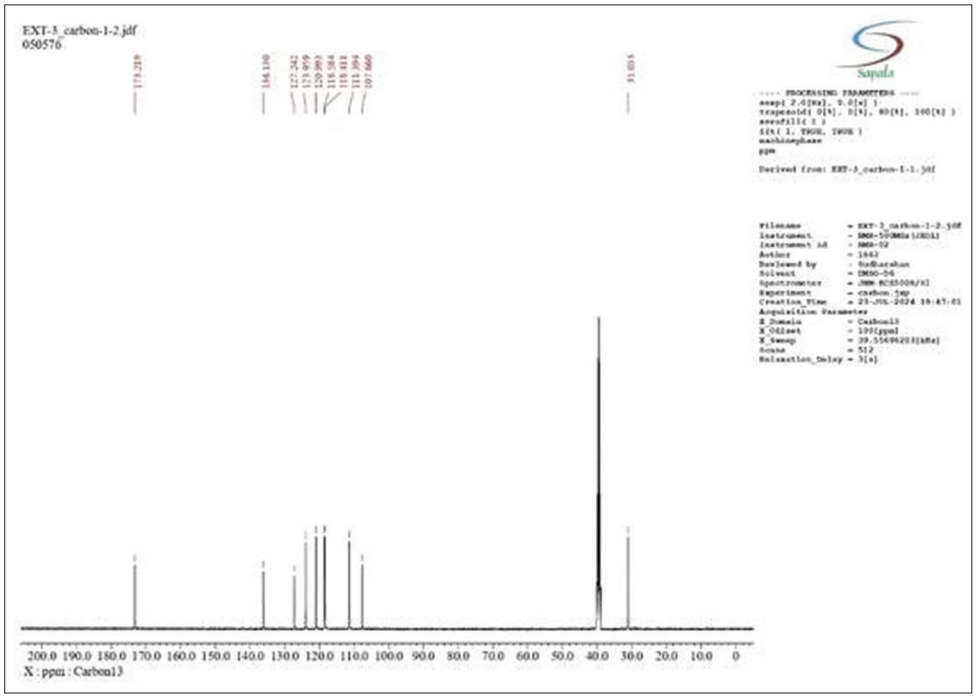


**Fig. 18: Carbon-13 nuclear magnetic resonance spectrum of component B**

$^{1}$H NMR (500 MHz in $CHCl_3$-$D_3$):δ 6.534 (1H, t, J=2Hz, H3), 7.191 (1H, dd, $J_1$=3Hz, $J_2$=2Hz, H2), 7.222 (1H, dd, $J_1$=8Hz, $J_2$=2Hz, H4), 7.503 (1H, d, J=8.5Hz, H5), 7.557 (1H, s, H6), 8.151 (1H, s, H1).

$^{13}$C NMR (500 MHz in $CHCl_3$-$D_3$):δ102.782, 113.926, 115.414, 121.893, 123.093, 124.763, 126.712, and 136.550.

Melting point of standard 6-Bromoindole was found to be 93–95℃

*Standard 6-bromoindole*

$^{1}$H NMR (500 MHz in $CDCl_3$):δ6.537 (1H, t, J=2Hz, H3), 7.188 (1H, dd, $J_1$=3Hz, $J_2$=2Hz, H2), 7.227 (1H, dd, $J_1$=8Hz, $J_2$=2Hz, H4), 7.506(1H, d, J=8.5Hz, H5), 7.553(1H, s, H6), 8.134 (1H, s, H1).

$^{13}$C NMR (500 MHz in $CDCl_3$):δ102.744, 113.917, 115.376, 121.883, 123.074, 124.782, 126.673, and 136.502.

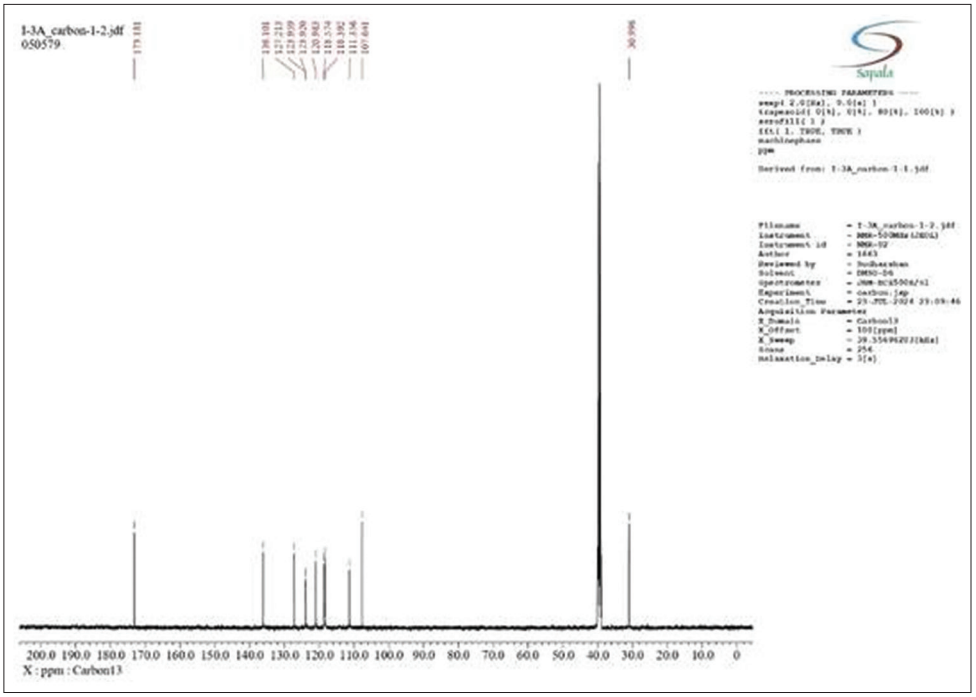


**Fig. 19: Carbon-13 nuclear magnetic resonance spectrum of standard indole-3-acetic acid**

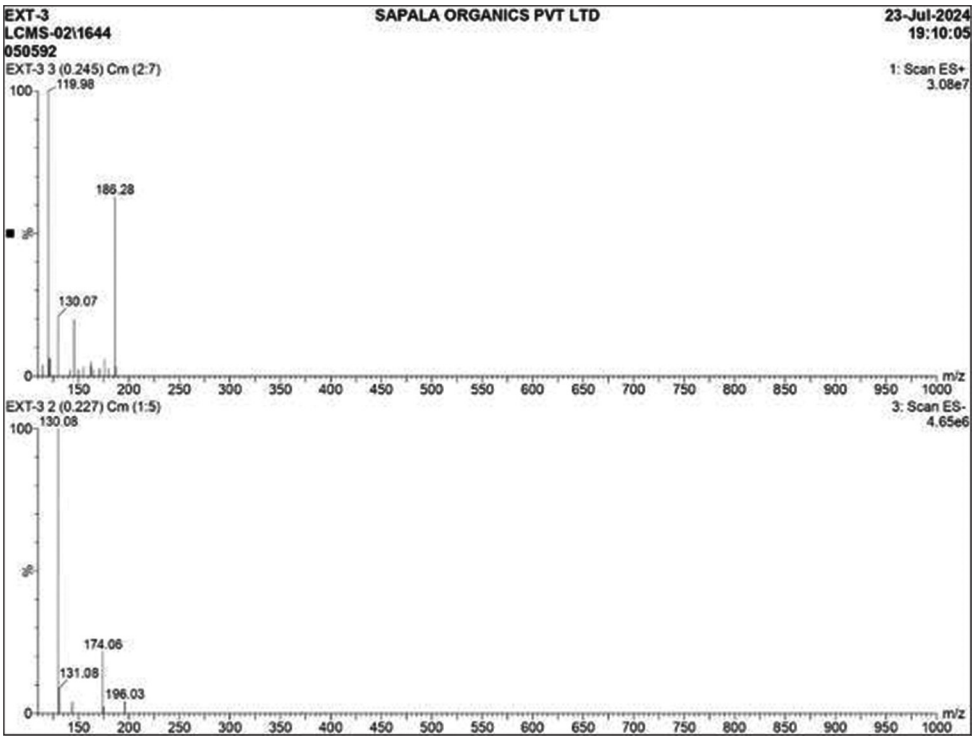


**Fig. 20: Mass spectrum of component B**

$^{1}$HNMR signals attributed to each hydrogen of component A (Fig. 3) with standard 6-bromoindole (Fig. 4) comply with the theoretical values as predicted by MestReNova. From the $^{13}$C NMR spectrum of component A (Fig. 5), it is evident that the δ ppm value of the C-6 atom is 115.414, which is lower in value than that of the 5, which is 121.893. As the C-6 is substituted with an electronegative bromine atom, it has a shielding effect, so the delta value is relatively in an upfield position with respect to C-5, which again justifies the position of the bromine atom in the compound. In the $^{13}$C NMR spectrum of standard 6-bromoindole (Fig. 6), the values of the C-6 and C-5 atoms are 115.376 and 121.883, respectively. The signals in the 113–126 ppm range confirm the presence of the indole ring structure.

Wave numbers between 4000 and 400 $cm^{-1}$ were used to record FTIR spectra. This is the FT-IR spectra of component A (Fig. 9). The N-H peak was identified as the source of the characteristic strong stretching vibration band that is visible at 3209.93 $cm^{-1}$. Due to the N-H distortion, the peak at 1605.45 $cm^{-1}$ is comparatively medium. The C-N stretching vibration is the cause of the sharp signal at 1335.46 $cm^{-1}$. It is possible to attribute the symmetric and asymmetric C-H stretching vibration

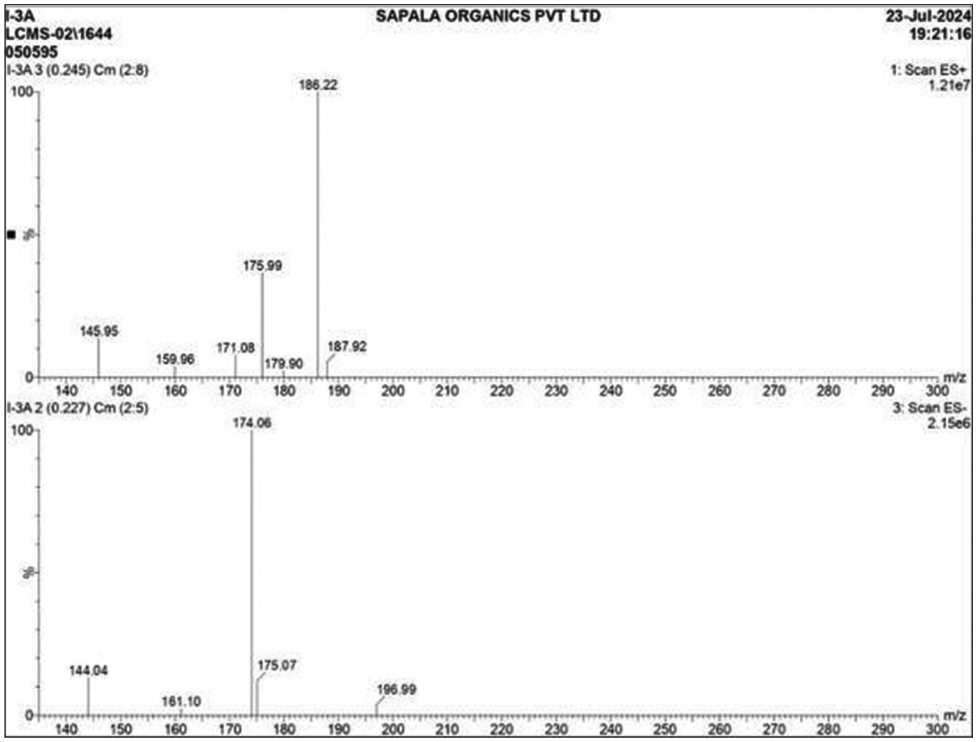


**Fig. 21: Mass spectrum of standard indole-3-acetic acid**

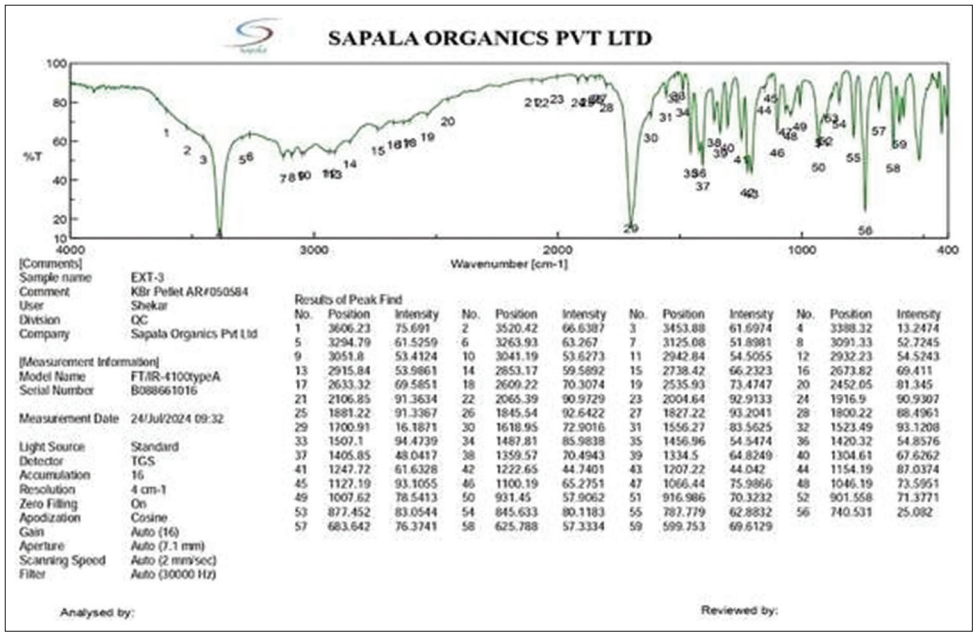


**Fig. 22: Fourier-transform infrared spectroscopy spectrum of component B**

peaks at 2932.23 $cm^{-1}$ and 3098.08 $cm^{-1}$. The sample exhibited the distinctive aromatic C=C strong stretching at 1520.6 $cm^{-1}$ and 1567.84 $cm^{-1}$. Peak vibrations at 1605.45 $cm^{-1}$ and 1446.35 $cm^{-1}$ were caused by the sample's C=C (in ring) stretching. Peaks of vibration 729.925 $cm^{-1}$ and 760.78 $cm^{-1}$ were caused by the control's =C-H out-of-plane deformation. Wave numbers 729.925 $cm^{-1}$ and 1167.69 $cm^{-1}$ are linked to the stretching vibration of C-Br.

The N-H peak of the standard 6-bromoindole (Fig. 10) was identified as the source of the strong stretching vibration band at 3209.93 $cm^{-1}$. Due to the N-H distortion, the peak at 1605.45 $cm^{-1}$ is comparatively medium. The C-N stretching vibration is the cause of the sharp signal at 1335.46 $cm^{-1}$. It is possible to assign the symmetric and asymmetric C-H stretching vibration peaks at 3032.51 $cm^{-1}$ and 3065.3 $cm^{-1}$. The sample exhibited the distinctive aromatic C=C strong stretching at 1520.6 $cm^{-1}$ and 1567.84 $cm^{-1}$. Peak vibrations at 1605.45 $cm^{-1}$ and 1446.35 $cm^{-1}$ were caused by the sample's C=C (in ring) stretching.

Vibration peaks 729.925 $cm^{-1}$and 760.78 $cm^{-1}$appeared due =C-H out-of-plane deformation in control. Wave numbers 1167.69 $cm^{-1}$ and 729.925 $cm^{-1}$ are associated with C-Br stretching vibration.

UV-visible spectra of **(**Fig. 11) the standard 6-bromoindole were recorded in methanol, and the $\lambda_{max}$ was observed at 266 nm. The

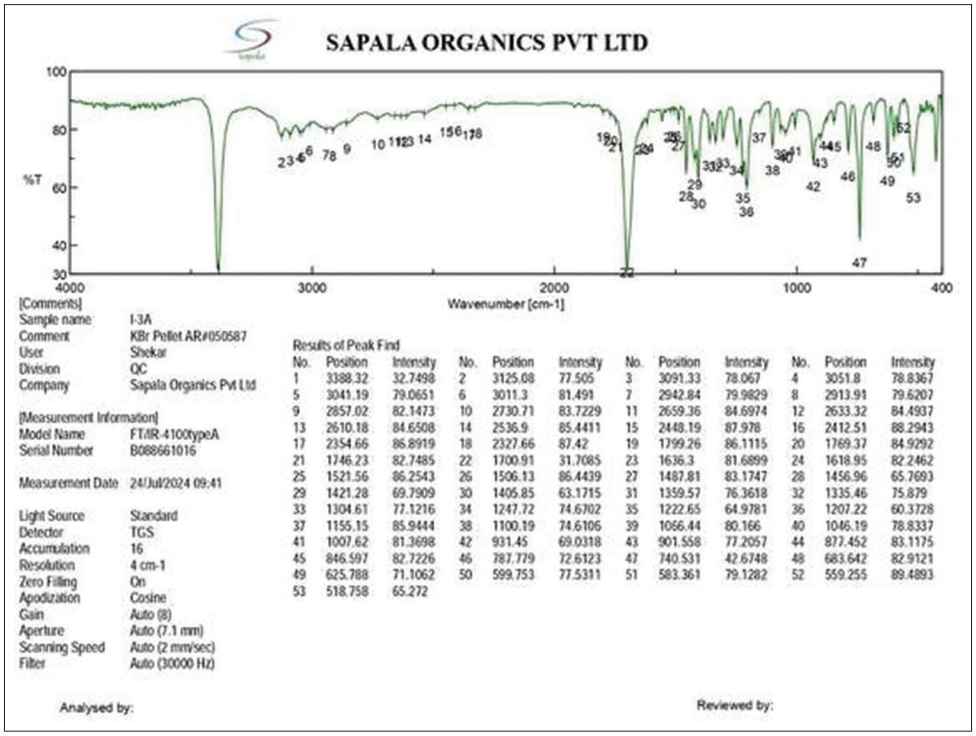


**Fig. 23: Fourier-transform infrared spectroscopy spectrum of standard indole-3-acetic acid**

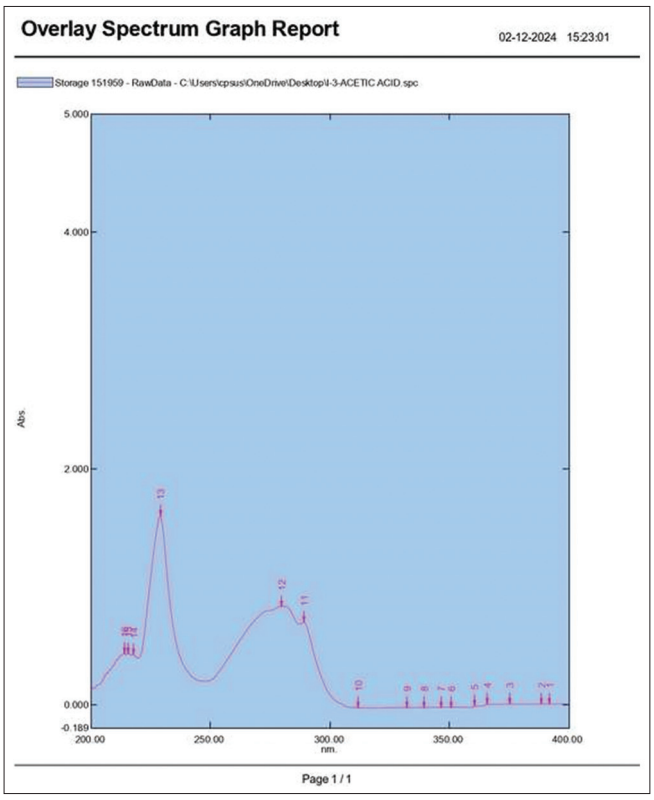


**Fig. 24: Ultraviolet spectrum of standard indole-3-acetic acid**

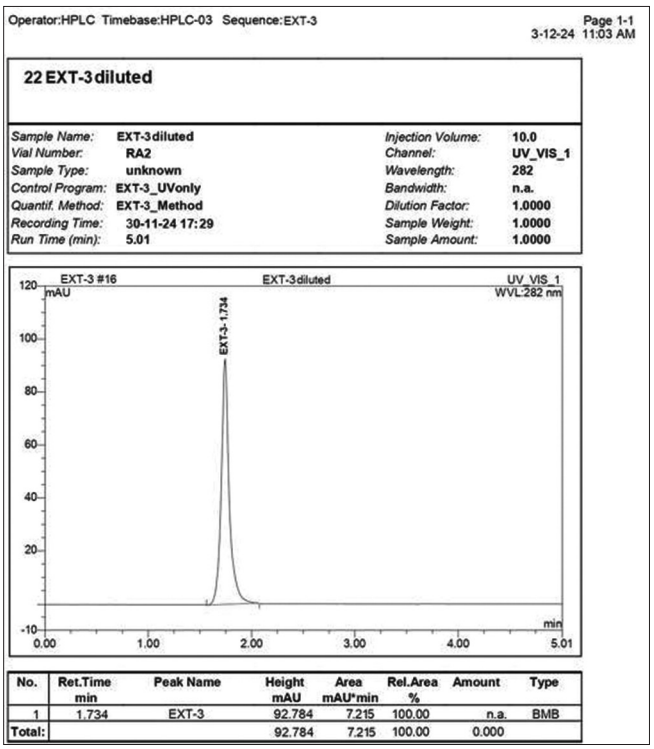


**Fig. 25: High-performance liquid chromatography peak of component B with Rt 1.734**

retention time in HPLC of the standard 6-bromoindole was found to be 2.113 (Fig. 13) and for the extract the Rt was 2.115 (Fig. 12). The area under the curve (AUC) shows that the extract was pure.

**Structural characterization of the component B**

The component B (Fig. 15), with $R_f$ value of 0.86, exhibited four peaks (m/z) at 130.08 ($C_9H_8O$), 131.08 ($C_9H_8O$+H), 174.06 ($M^+$) and 196.03 (M+Na) (Fig. 20). Following the same methodology different databases were searched for the probable compound with molecular weight of approximately 174.06 and we retrieved six possible structures, namely, Indole-3-acetic acid, (E)-2-((E)-3-(Hydroxyimino)butan-2-ylidene) hydrazinecarbimidothioicacid,(E)-Diethyl diazene-1,2-dicarboxylate, Diallyl(chloromethyl)(methyl)silane, 1,3-Dimethylisophosphinoline, and 3,6-bis(hydroxymethyl)-3,6-dihydropyrazine-2,5-diol (Fig. 14).

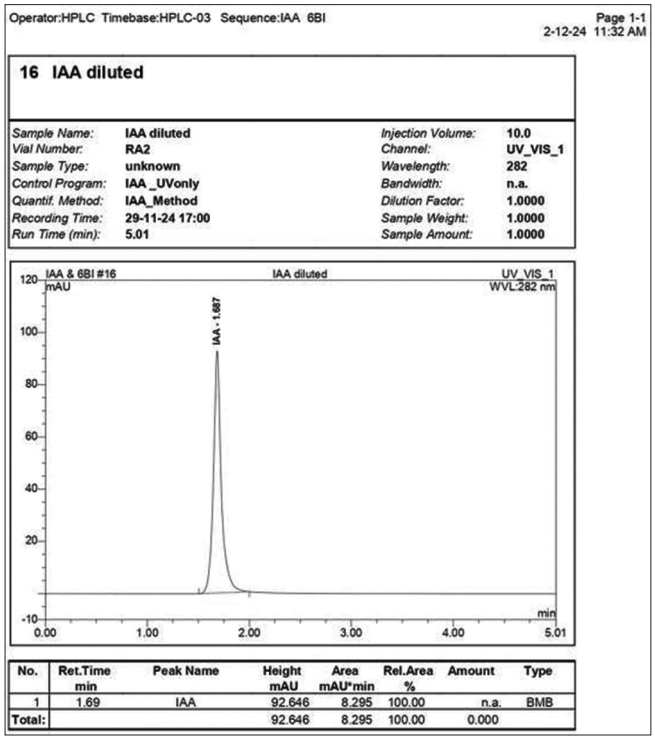


**Fig. 26: High-performance liquid chromatography peak of standard indole-3-acetic acid with Rt 1.687**

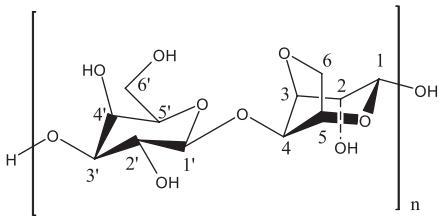


**Fig. 27: Structure of the repeating units of agarose as polymer**

Spectral data for component B (Fig. 15) was collected and matched with the probable compounds. The $^{1}$HNMR data show that component B (Fig. 16) is indole-3-acetic acid. The interpretation of the spectral data is given below.

*Component B*

$^{1}$HNMR (500MHz in DMSO-D6): δ3.630 (2H, s, H4, H5), 6.976 (1H, t, J=7.5 Hz, H7), 7.069 (1H, t, J=7Hz, H8), 7.221 (1H, d, J=2Hz, H2), 7.344 (1H, d, J=8 Hz, H9), 7.488 (1H, d, J=7.5Hz, H6), 10.902 (1H, s, H1), 12.136 (1H, s, H3).

$^{13}$C NMR (500 MHz in $CHCl_3$-$D_3$): δ31.053, 107.660, 111.394, 118.411, 118.584, 120.993, 123.959, 127.242, 136.130, and 173.219.

Standard indole-3-acetic acid

$^{1}$HNMR (500 MHz in DMSO-D6): δ3.632 (2H, s, H4, H5), 6.961 (1H, t, J=7Hz, H7), 7.071 (1H, t, J=7Hz, H8), 7.223(1H, d, J=2Hz, H2), 7.345(1H, d, J=7.5Hz, H9), 7.489(1H, d, J=7.5Hz, H6), 10.898 (1H, s, H1), 12.137 (1H, s, H3).

$^{13}$C NMR (500 MHz in $CHCl_3$-$D_3$): δ30.996, 107.641, 111.356, 118.392, 118.574, 120.983, 123.920, 123.959, 127.213, 136.101, and 173.181.

$^{1}$HNMR signals attributed to each hydrogen of component B (Fig. 16) comply with the theoretical values predicted by MestReNova and that of standard Indole-3-acetic acid (Fig. 17). From the $^{13}$C NMR spectrum, it is evident that the signals in the 111–126 δ ppm range confirm the presence of the indole ring structure. The signal at 31.053 ppm and 173.219 δ ppm ranges confirm the presence of the acetic acid side chain, including the methylene and carbonyl groups. The appearance of relatively broad signals in the range of ~110–130 ppm reflects the aromatic nature of the indole ring. The signals for the standard Indole-3-acetic acid (Fig. 19) are correlated with the component B (Fig. 18). The Standard Indole-3-acetic acid exhibited two peaks (m/z)174.06 (M+) and 196.99 (M+Na) (Fig. 21) molecular weight of standard almost matches with the component B.

The IR spectrum of the component B (Fig. 22) reveals a sharp band at 3388.32 $cm^{-1}$, attributed to indole -NH-, alongside a succession of bands ranging from 2738.42 to 3125.08 $cm^{-1}$, corresponding to hydrogen-bonded -OH stretching frequencies. A pronounced peak at 1700.91 $cm^{-1}$ resulted from C=O stretching vibrations of the carboxylic group. The absorbance of broad bands between 3091.33 and 3125.08 $cm^{-1}$, along

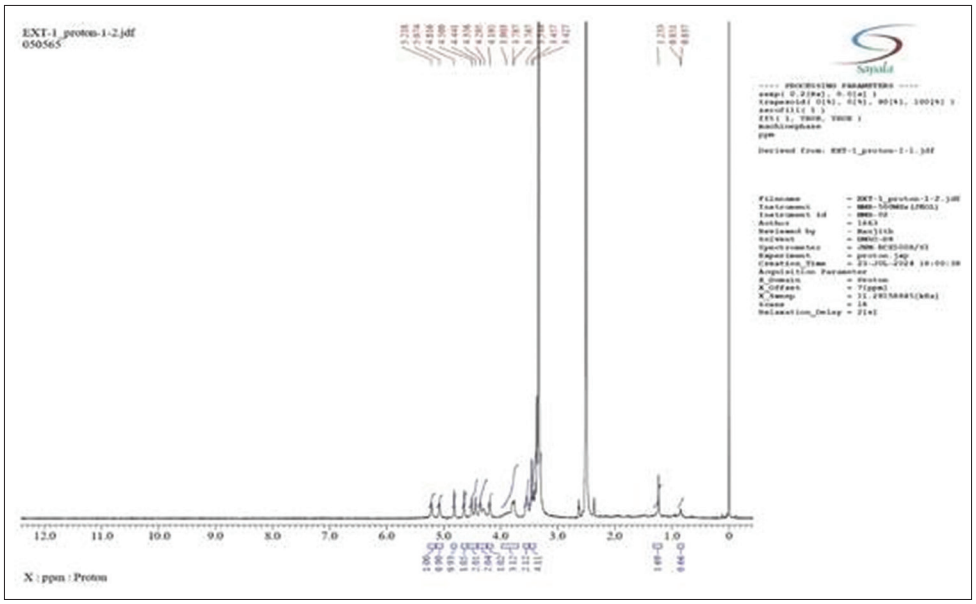


**Fig. 28: Proton nuclear magnetic resonance spectrum of extracted agarose**

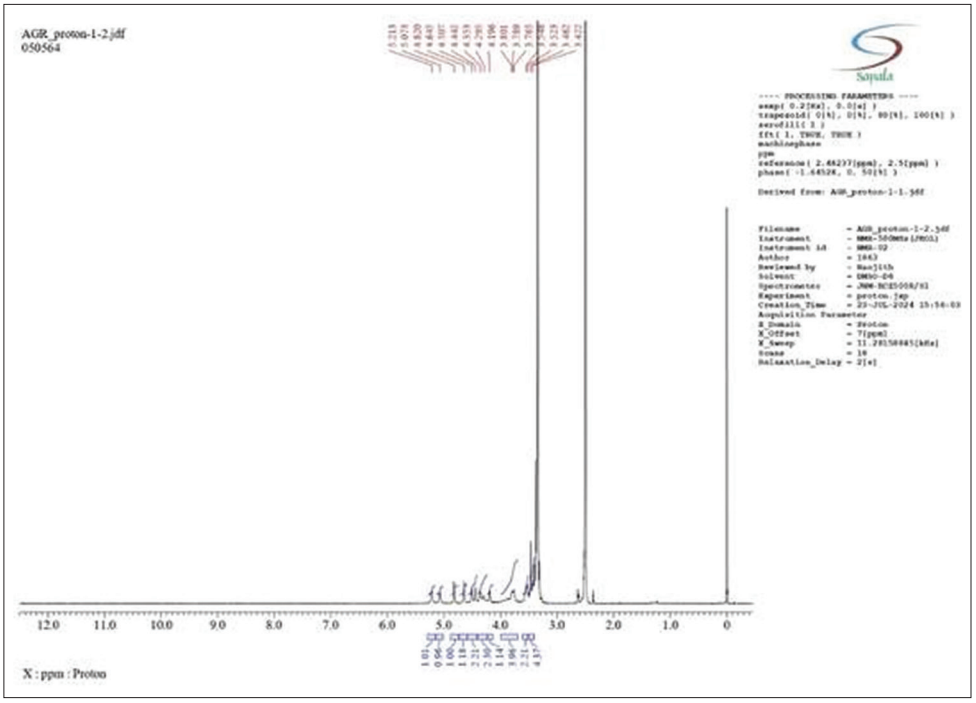


**Fig. 29: Proton nuclear magnetic resonance spectrum of standard agarose**

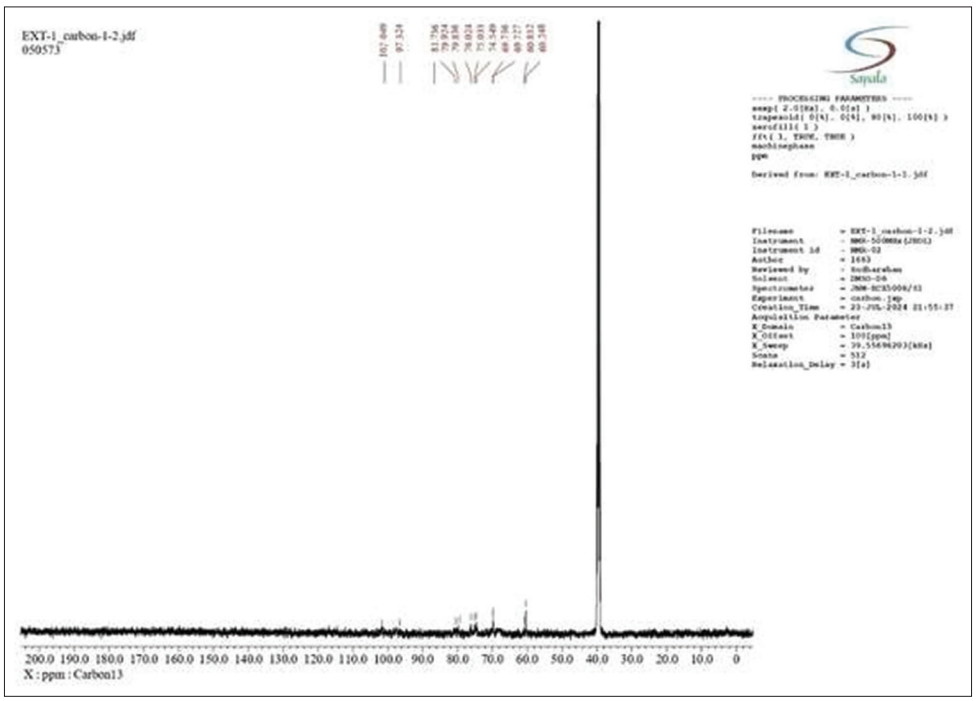


**Fig. 30: Carbon-13 nuclear magnetic resonance spectrum of extracted agarose**

with a singular intense sharp band at 3388.32 $cm^{-1}$, corroborates the absence of free -$NH_2$ and the presence of the indole-NH-group.

The IR spectrum of the standard Indole-3-acetic acid (Fig. 23) reveals a sharp band at 3388.32 $cm^{-1}$, attributed to indole -NH-, alongside a succession of bands ranging from 2730.71 to 3125.08 $cm^{-1}$, corresponding to hydrogen-bonded -OH stretching frequencies. A pronounced peak at 1700.91 $cm^{-1}$ resulted from C=O stretching vibrations of the carboxylic group. The absorbance of broad bands between 3091.33 and 3125.08 $cm^{-1}$, along with a singular intense sharp band at 3388.32 $cm^{-1}$, corroborates the absence of free -$NH_2$ and the presence of the indole-NH-group.

The UV-visible spectra of the extract and the standard were recorded in methanol, and the λmax was observed at 282 nm (Fig. 24). The retention time in HPLC of the standard Indole-3-Acetic acid was found to be 1.687 (Fig. 26), and for the component B, the Rt was 1.734 (Fig. 25). The AUC shows that the extract was pure.

**Structural characterization of agarose from agar**

With a molecular weight of roughly 120,000 Dalton, agarose is a linear polymer made up of alternating D-galactose and 3,6-anhydro-L-galactopyranose connected by α-(1→3) and β-(1→4) glycosidic linkages. The two units are designated here as G which is 1,3-β-D-

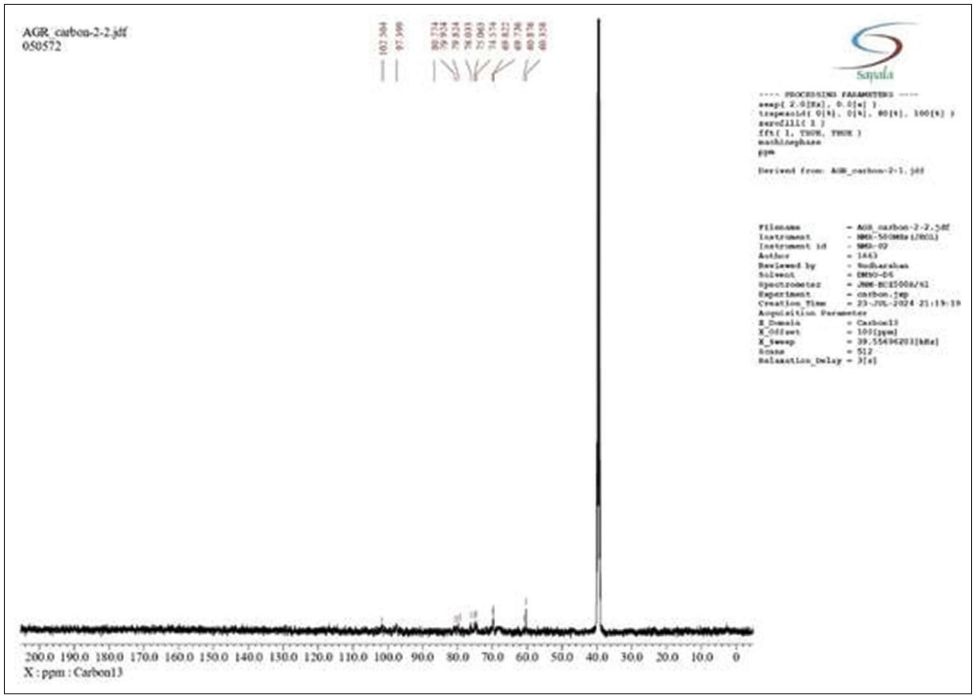


**Fig. 31: Carbon-13 nuclear magnetic resonance spectrum of standard agarose**

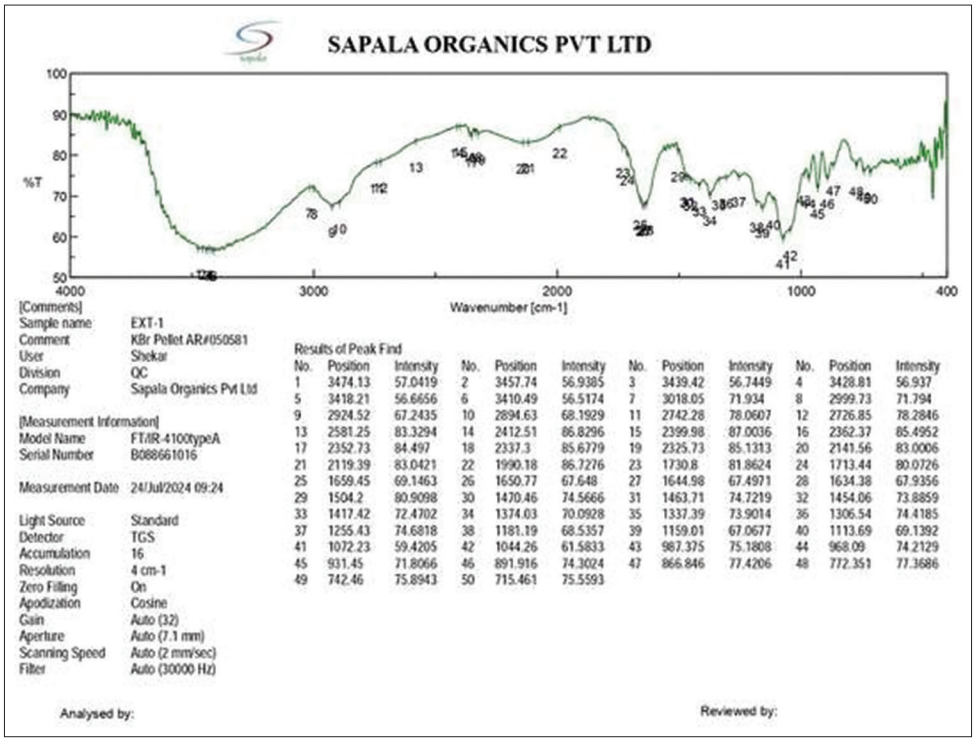


**Fig. 32: Fourier-transform infrared spectroscopy spectrum of extracted agarose**

galactose, and A which is 1,4-α-L-3-6-anhydrogalactose (Fig. 27). Analytical testing and comparison with a reference agarose proved the structural integrity and purity of the extracted agarose.[1]H NMR (Fig. 28) and [13]C NMR (Fig. 27) spectra of extracted and reference agarose (Figs. 29 and 31) performed in DMSO-*d*6 solvent at 70°C are compared.

At δ (in ppm)=C1'-5.073, C1-5.213, and for agarose skeleton with 18 hydrogens (C2-C6) and (C2'-C6') - 3.422–4.820, standard agarose exhibits peaks [34] in [1]HNMR (Fig. 29), whereas the extracted agarose (Fig. 30) exhibits peaks at C1'-5.074, C1-5.218, and for agarose skeleton with 18 hydrogens (C2-C6) and (C2'-C6') - 3.427–4.816.

Table 1 presented a comparison of the [13]C NMR chemical shifts between the standard and extracted agarose. The values can be well correlated with the structures.

The FTIR spectra indicated that the diagnostic signals of the isolated agarose correspond with the structure of the standard substance. The characteristic dips of standard agarose (Fig. 33) in the IR spectrum at

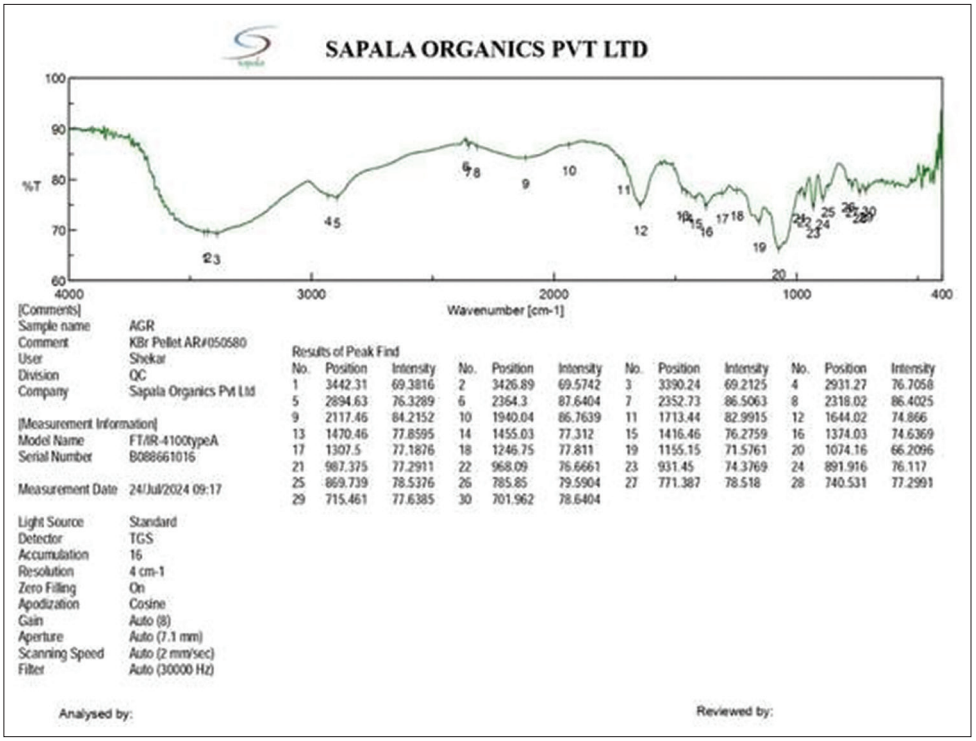


**Fig. 33: Fourier-transform infrared spectroscopy spectrum of standard agarose**

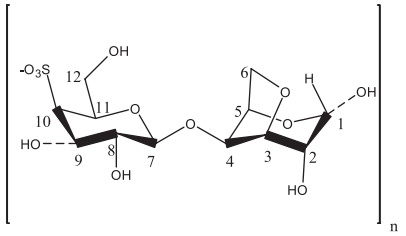

β-D-galactose-4-sulfate (G4S) 3,6-anhydro-α-D-galactose (AnGal)

**Fig. 34: Structure of the repeating units of carrageenan as polymer**

**Table 1: Comparison of chemical shifts between standard (Fig. 31) and extracted agarose (Fig. 30) in $^{13}$C NMR**

| Source | Unit | $^{13}$C NMR chemical shift (in ppm) | | | | | |
|---|---|---|---|---|---|---|---|
| | | C-1 | C-2 | C-3 | C-4 | C-5 | C-6 |
| Standard agarose | G | 102.504 | 74.574 | 80.774 | 60.876 | 75.063 | 60.358 |
| | A | 97.399 | 69.822 | 79.924 | 79.824 | 76.033 | 69.736 |
| Extracted agarose | G | 102.049 | 74.549 | 81.736 | 69.727 | 76.024 | 60.248 |
| | A | 97.324 | 69.736 | 79.924 | 79.836 | 75.033 | 60.832 |

$^{13}$C NMR: Carbon-13 nuclear magnetic resonance

771.387, 891.916, and 931.45 cm$^{-1}$, attributed to the 3,6-anhydro-β-galactose skeleton, and at 1155.15 and 1074.16 cm$^{-1}$, corresponding to the -C-O-C- and glycosidic linkages, respectively, are observed in the extracted agarose (Fig. 32) at 772.351, 891.916, 931.45, 1159.01, and 1072.23 cm$^{-1}$. The signal intensity elucidates their complete purity.

The molecular weight of a repeating unit of agarose is approximately 630.5 Daltons. Commercial samples generally fall within the 80,000 to 140,000 molecular weight range. Certain investigations indicate that laboratory-extracted agarose-type polysaccharides may possess reduced molecular weights. The difficulty of interpreting the mass spectra of high molecular polymers has hindered this study.

**Structural characterization of carrageenan**

Carrageenan's are a family of high molecular weight natural linear sulfated polysaccharides found in the cell walls of red algae. There are mainly three types of carrageenan, namely, kappa, iota, and lambda. They differ in their sulfation level, that is, kappa carrageenan bears one sulfate group while iota and lambda bear two and three sulfate groups, respectively. Kappa and iota bear anhydro bridges, while lambda has no anhydro bridge.

The standard carrageenan (Fig. 34) demonstrates the presence of anomeric protons at the AnaGl subunit and G4s H-1 and H-1′, with chemical shift values of δ ppm 5.201 and 5.092, respectively [35,37]. The multiplet ring protons of H-2 to H-6 in the G4S and AnGal subunits exhibit peaks ranging from 4.769 to 4.354 ppm (Fig.36). This value confirms the presence of sulfated galactose units and 3,6-anhydro bridges, indicating the existence of kappa carrageenan. Significant peaks in the range of 3.438 to 3.007 correspond to overlapping H-2 to H-6 protons from various sugar residues. A comparable signal pattern was detected in the carrageenan extract. The signals from the extracted carrageenan indicate the presence of anomeric protons at the AnaGl subunit and G4s H-1 and H-1′, with chemical shift values of δ ppm 5.218 and 5.120, respectively. The ring protons H-2 to H-6 of the G4S and AnGal subunits are responsible for regions exhibiting peaks between 4.767 and 4.353 ppm (Fig.35). This value indicates the existence of sulfated galactose units and 3,6-anhydro bridges, confirming the presence of kappa carrageenan. Sulfation induces downfield shifts to 4.8 ppm. Significant peaks at 3.438-3.018 indicate the overlap of H-2 to H-6 protons from various sugar residues.

The **(**Fig. 38) shows the $^{13}$C NMR spectra for twelve carbons of standard carrageenan, where $^{13}$C NMR (DMSO-D6), δ=102.249 (C′-1), δ=95.102 (C1), δ=80.956 (C′-3), δ=79.921 (C3), δ=79.726 (C4), δ=76.067 (C5), δ=75.036 (C′-5), δ=74.040 (C′-4), δ=69.724 (C′-2), δ=69.667 (C-2), δ=69.321 (C-6), and δ=61.236 (C′-6). These peaks agree with the reported value as in Abu Bakar, Azeman, Mobarak, Mokhtar, Bakar and Yun-Peng, Xi-Kun, Xiu-Fang *et al*., which confirms the κ-carrageenan nature of the extracted sample (Fig. 37) [36,38]. Table 2 presented a comparison of the $^{13}$C NMR chemical shifts between the standard and

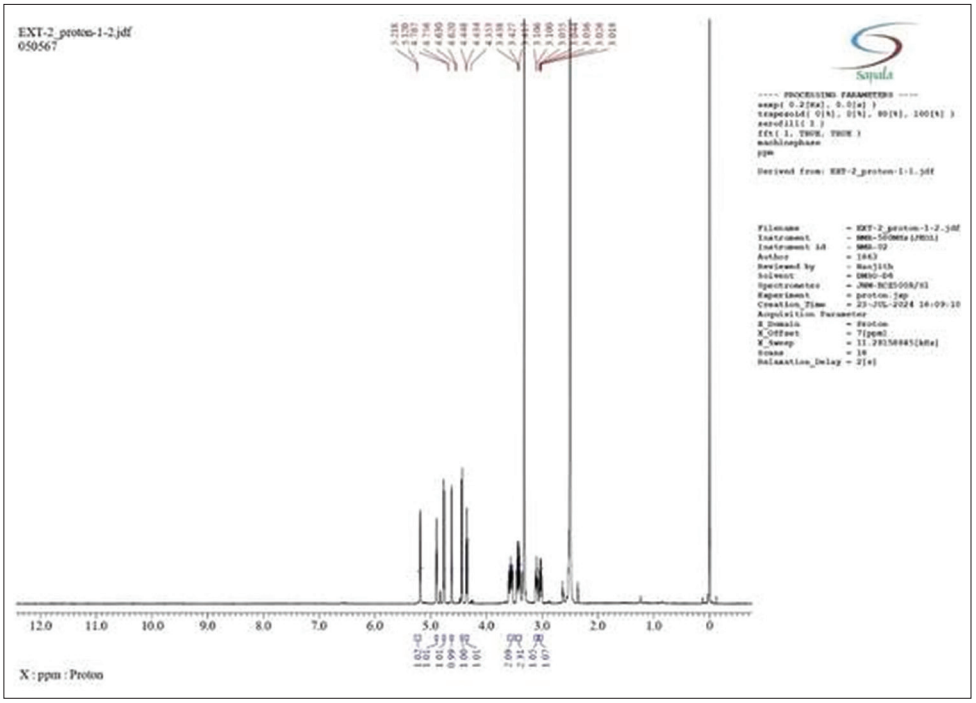


**Fig. 35: Proton nuclear magnetic resonance spectrum of extracted carrageenan**

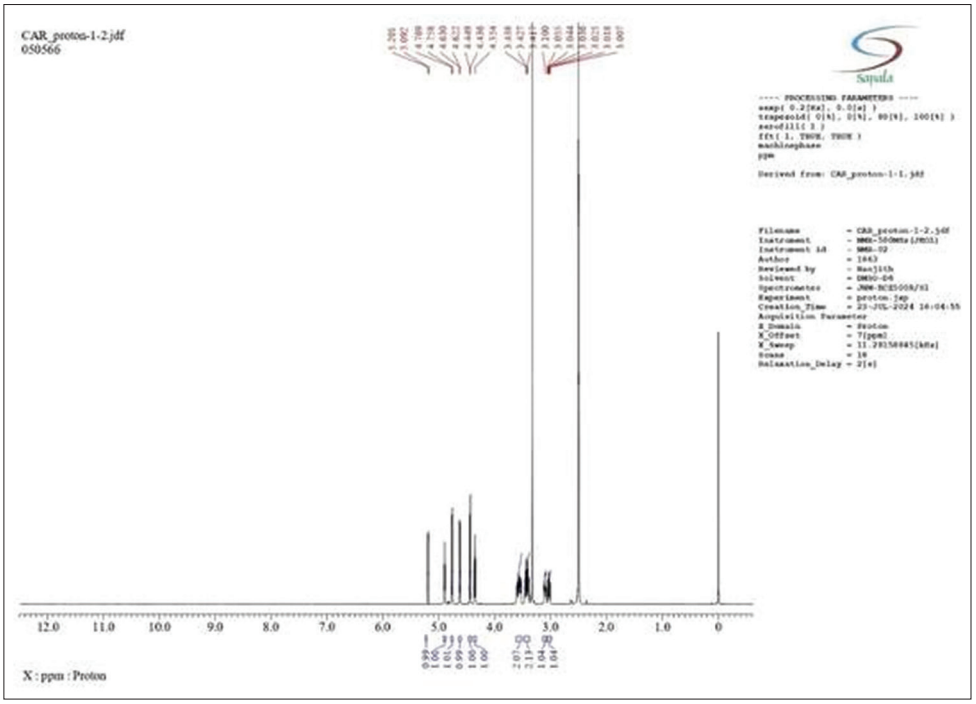


**Fig. 36: Proton nuclear magnetic resonance spectrum of standard carrageenan**

**Table 2: $^{13}$C NMR chemical shift comparison of the standard and extracted carrageenan**

| Sample | Unit | $^{13}$C NMR chemical shift (in ppm) | | | | | |
|---|---|---|---|---|---|---|---|
| | | C-1 | C-2 | C-3 | C-4 | C-5 | C-6 |
| Standard carrageenan | G4S | 102.249 | 69.724 | 80.956 | 74.040 | 75.036 | 61.236 |
| | AnGal | 95.102 | 69.667 | 79.921 | 79.726 | 76.067 | 69.321 |
| Extracted carrageenan | G4S | 102.236 | 69.731 | 80.954 | 74.011 | 75.020 | 61.240 |
| | AnGal | 95.232 | 69.654 | 79.901 | 79.740 | 76.024 | 69.201 |

$^{13}$C NMR: Carbon-13 nuclear magnetic resonance

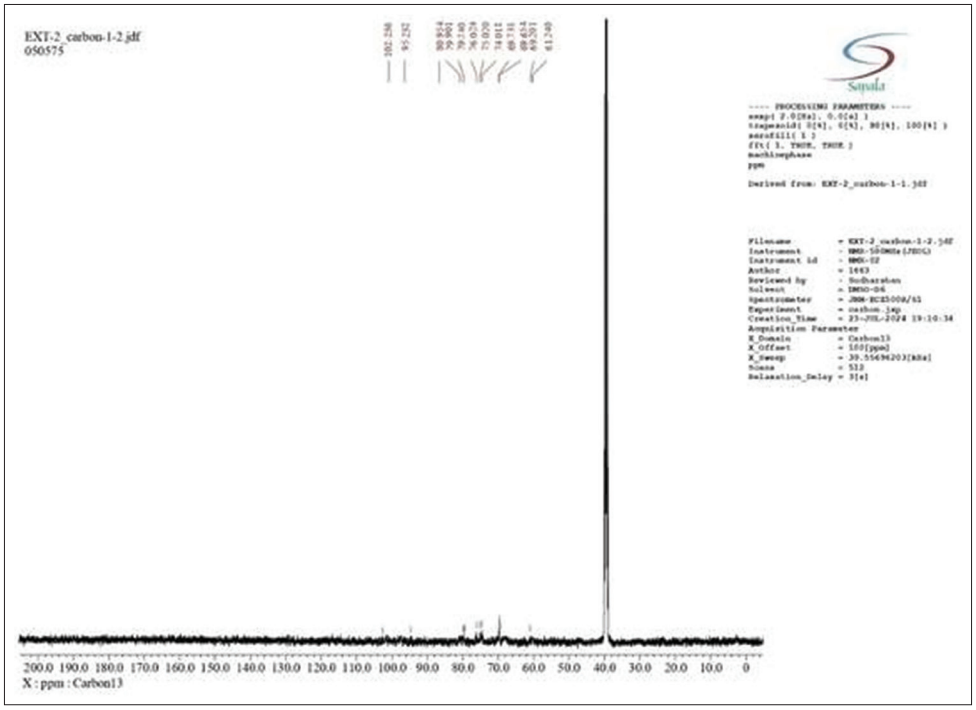


**Fig. 37: Carbon-13 nuclear magnetic resonance spectrum of extracted carrageenan**

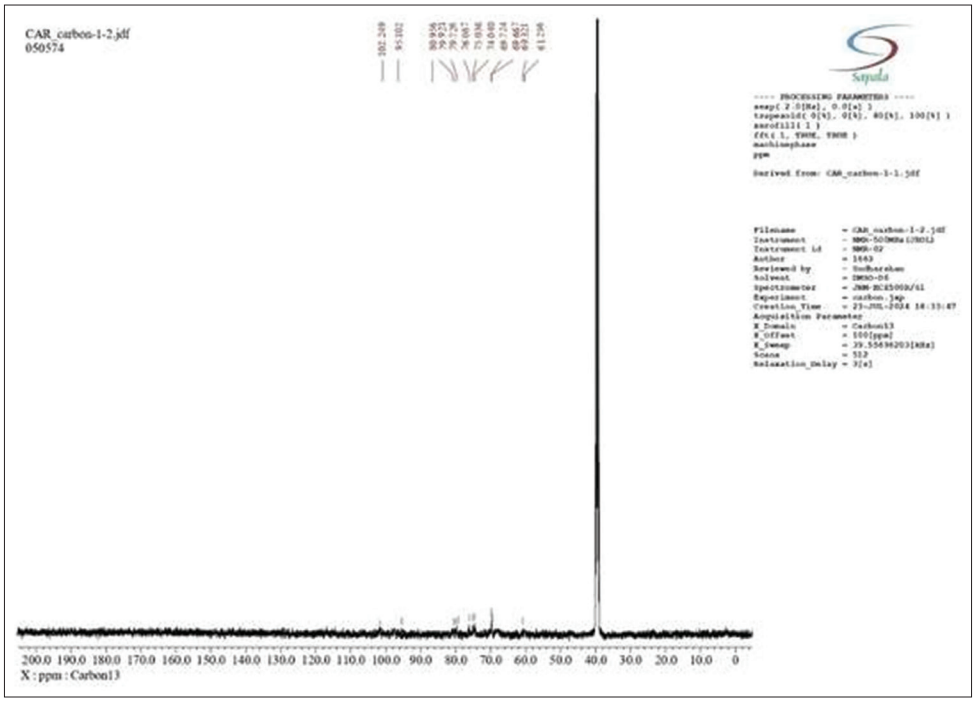


**Fig. 38: Carbon-13 nuclear magnetic resonance spectrum of standard carrageenan**

extracted carrageenan. The values can be well correlated with the structures.

The standard spectrum of carrageenan (Fig. 40) displays characteristic peaks at 1255.43 $cm^{-1}$ and 868.774 $cm^{-1}$, which correspond to the symmetric vibration of O=S=O and the stretching vibration of C4–O–S, respectively. In the meantime, the presence of C–O, C–H, and broad O–H stretches in standard carrageenan was noted at approximately 1048.12 $cm^{-1}$, 2924.52 $cm^{-1}$, and 3364.21 $cm^{-1}$, respectively. The peak identified at 931.45 $cm^{-1}$ corresponds to the C–O–C bond in 3,6-anhydrous-D-galactose.

The extracted carrageenan (Fig. 39) exhibited characteristic peaks at 1252.54 $cm^{-1}$ and 851.418 $cm^{-1}$, corresponding to the O=S=O symmetric vibration and C4–O–S stretching vibration, respectively. In the meantime, the presence of C–O, C–H, and broad O–H stretches in the extracted carrageenan was noted at approximately 1051.01 $cm^{-1}$, 2934.16 $cm^{-1}$, and 3394.1 $cm^{-1}$, respectively. The peak identified at 916.022 $cm^{-1}$ corresponds to the C–O–C bond in 3,6-anhydrous-D-galactose.

**Anticancer activity of the extracts and the isolates on A549 NSCLC cell line**

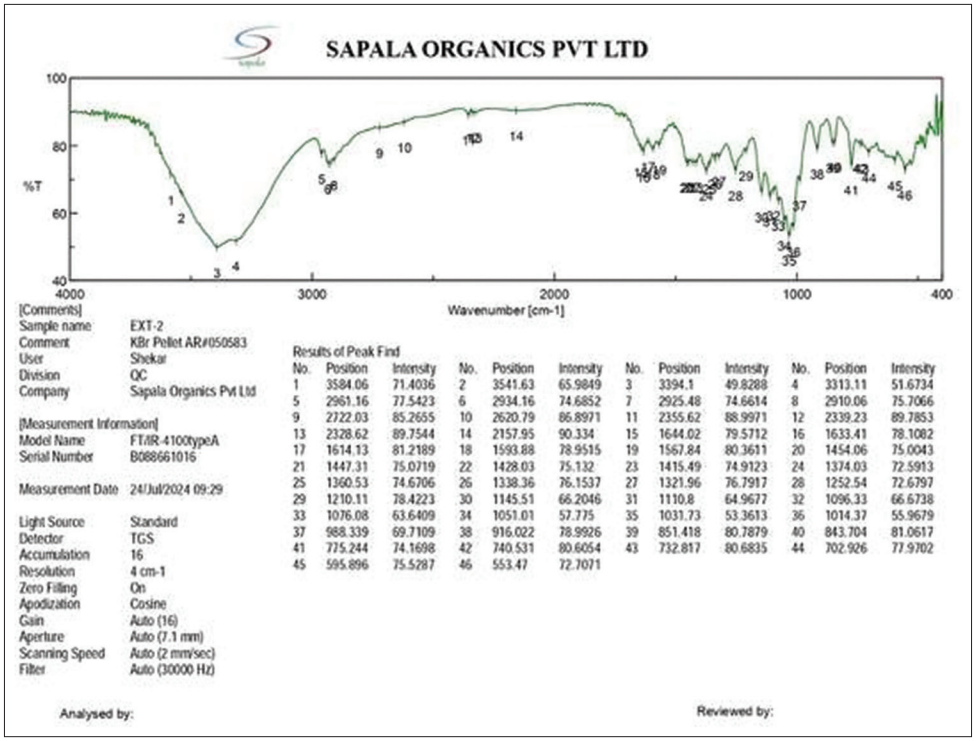


**Fig. 39: Fourier-transform infrared spectroscopy spectrum of extracted carrageenan**

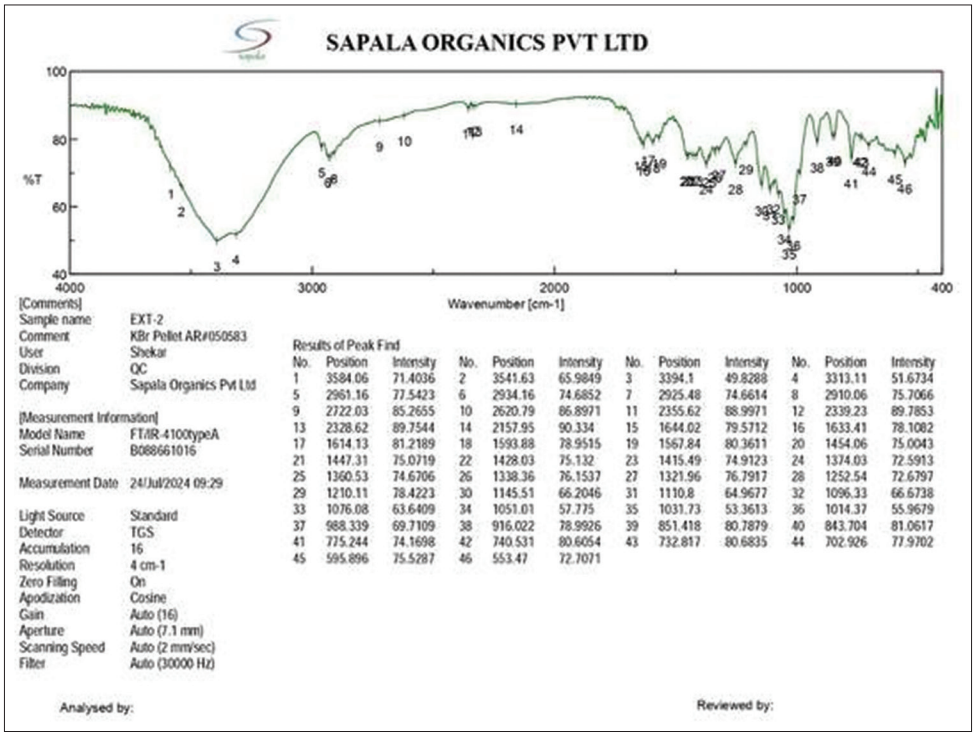


**Fig. 40: Fourier-transform infrared spectroscopy spectrum of standard carrageenan**

Based on the MTT assay results (Table 3), it was found that the A549 cell line did not exhibit any encouraging cytotoxic activity when exposed to varying doses of the three distinct extracts. The standard doxorubicin was found to be 266 µg/mL. The $IC_{50}$ values for the aqueous, methanol, and ethanol extracts were 967.8, 733.4, and 998 g/mL, respectively. 6-Bromoindole and Indole-3-acetic acid showed more than 10000 µg/mL.

**Anti-fungal activity of the extracts and isolates by zone inhibition method**

Table 4 indicates the values of the zone of inhibition (in mm) of the three extracts and two isolated compounds. Standard amphotericin B had an effect of 13 mm, while the ethanol extract had strong antifungal activity at 11.4 mm, and indole-3-acetic acid followed with 9.9 mm. 6-bromo indole measured 1.5 mm, and the aqueous extract was at 4.8 mm. 6-bromo indole exhibited a measurement of 1.5 mm, while the aqueous extract

**Table 3: $IC_{50}$ values of the different extracts and compounds tested on A549 non-small cell lung cancer cell line in triplicate**

| S. No. | Sample | $IC_{50}$ value (in µg/mL) [a] Mean±SD |
|---|---|---|
| 1. | Aqueous extract | 967.8±0.193 |
| 2. | Methanol extract | 733.4±0.099 |
| 3. | Ethanol extract | 998.1±0.283 |
| 4. | 6-Bromoindole | >1000 |
| 5. | Indole-3-acetic acid | >1000 |
| 6. | Doxorubicin (standard) | 266.6±0.093 |

[a]Results are the average of three separate experiments and represented as±SD (standard deviation). $IC_{50}$: 50% inhibitory concentration

**Table 4: MOZI mean values of the different extracts and isolates tested on *Candida albicans* in triplicate**

| S. No. | Sample | MZOI (in mm) Mean±SD | Amount loaded (µg) |
|---|---|---|---|
| 1. | Aqueous extract | 4.8±0.67 | 10 µL from 0 to 200 µg/disc |
| 2. | Methanol extract | 9.7±0.55 | 10 µL from 0 to 200 µg/disc |
| 3. | Ethanol extract | 11.4±0.32 | 10 µL from 0 to 200 µg/disc |
| 4. | 6-Bromo indole | 1.5±0.87 | 10 µL from 0 to 200 µg/disc |
| 5. | Indole-3-acetic acid | 9.9±0.49 | 10 µL from 0 to 200 µg/disc |
| 6. | Amphotericin B (PC) standard | 13±0.23 | 50 |

MZOI: Maximum zone of inhibition, SD: Standard deviation

measured 4.8 mm. κ-carrageenan was found to have good antifungal activity (80%) against *C. albicans* in a range of 400–500 µg/mL of fungicidal concentration [39]. Agarose is used as a support structure for microbial growth, and hence it is not tested for antifungal activity.

**Statistical analysis**

$IC_{50}$ values (µG/mL) were calculated by fitting a sigmoidal dose-response curve (four-parameter logistic model) to the percentage inhibition data using GraphPad Prism-6 (GraphPad Software, Inc.). Each experiment was performed in triplicate, and the mean $IC_{50}$ value±SD was reported.

To determine the MZOI, the diameter of the clear area around the test substance was measured with a caliper. The mean ZOI for the given concentration was calculated by summing the ZOI values for all replicates and dividing by the number of replicates. The maximum ZOI is the largest mean value±SD ZOI observed across all the replicates.

## CONCLUSION

The aforementioned studies indicate that the three extracts of *P. subtilissima* Montagne exhibited no anticancer activity against the A549 lung carcinoma cell line; however, they demonstrated moderate efficacy against *C. albicans* by displaying antifungal properties when compared to the commercially available standard drug amphotericin B. Agarose was derived from agar, which was initially obtained from the *P. subtilissima* Montagne. Carrageenan was isolated, and both polysaccharides were characterized using spectrum analysis. 6-Bromoindole was isolated and identified as a prevalent precursor for the production of secondary metabolites in red algae. Indole-3-acetic acid was extracted and recognized as a growth hormone, with increased levels observed during its primary harvesting period. In this little timeframe of research, we ascertain that agarose and carrageenan were identified as anticipated in other red algae, while 6-bromoindole and indole-3-acetic acid were detected in abundance in *P. subtilissima* Montagne; nonetheless, more secondary metabolites likely exist that have not yet been studied.

## ACKNOWLEDGMENTS

The authors express their gratitude to the institution and university departments for their technical and moral assistance in successfully carrying out the project.

## AUTHORS' CONTRIBUTIONS

All the authors have contributed equally.

## CONFLICTS OF INTEREST

The authors declare that there is no conflicts of interest.

## FUNDING

The projected was completely funded by the authors.

## REFERENCES

1. Choudhury R, Sahoo N. Phytochemical evaluation and bioactivity of *Polysiphonia subtilissima* montagne. Asian J Chem. 2024 Aug 30;36(9):2083-8. doi: 10.14233/ajchem.2024.32122
2. Molecular Weight Search. Available from: https://webbook.nist.gov/chemistry/mw-ser [Last accessed on 2024 Jul 15].
3. Poynton EF, van Santen JA, Pin M, Contreras MM, McMann E, Parra J, *et al*. The natural products Atlas 3.0: Extending the database of microbially derived natural products. Nucleic Acids Res. 2025;53(D1):D691-9. doi: 10.1093/nar/gkae1093, PMID 39588755
4. Zhao H, Yang Y, Shuaiqi W. NPASS database update 2023: Quantitative natural product activity and species source database for biomedical research. Nucleic Acids Res. 2022 Nov 29;51(1):D621-8. doi: 10.1093/nar/gkac1069
5. Available from: https://chemdata.nist.gov/dokuwiki/doku.php?id=chemdata: msms [Last accessed on 2024 Aug 15].
6. AIST. Spectral Database for Organic Compounds, SDBS. Available from: https://sdbs.db.aist.go.jp [Last accessed on 2024 Aug 15].
7. Wang M, Carver JJ, Phelan VV, Sanchez LM, Garg N, Peng Y, *et al.* Sharing and community curation of mass spectrometry data with Global Natural Products Social Molecular Networking. Nat Biotechnol. 2016 Aug 9;34(8):828-37. doi: 10.1038/nbt.3597, PMID 27504778
8. Available from: https://pubchem.ncbi.nlm.nih.gov [Last accessed on 2024 Aug 15].
9. ChemSpider. Available from: https://www.chemspider.com/structuresearch [Last accessed on 2024 Aug 15].
10. Zdrazil B, Felix E, Hunter F, Manners EJ, Blackshaw J, Corbett S, *et al*. The ChEMBL Database in 2023: A drug discovery platform spanning multiple bioactivity data types and time periods. Nucleic Acids Res. 2024 Jan 5;52(D1):D1180-92. doi: 10.1093/nar/gkad1004, PMID 37933841
11. Irwin JJ, Tang KG, Young J, Dandarchuluun C, Wong BR, Khurelbaatar M, *et al*. ZINC20-A free ultra large-scale chemical database for ligand discovery. J Chem Inf Model. 2020 Oct 29;60(12):6065-73. doi: 10.1021/acs.jcim.0c00675, PMID 33118813
12. Guiry MD, Guiry GM. AlgaeBase: An on-line resource for Algae. Algae base. Cryptogam Algologie. 2014 May 30;35(2):105-15.
13. Lyu C, Chen T, Qiang B, Liu N, Wang H, Zhang L, *et al*. LCMNPD: A comprehensive marine natural products database towards facilitating drug discovery from the ocean. Nucleic Acids Res. 2021 Jan 8;49(D1):D509-15. doi: 10.1093/nar/gkaa763, PMID 32986829
14. Elsie BH, Dhanarajan MS, Sudha PN. N*vitro* screening of secondary metabolites and antimicrobial activities of ethanol and acetone extracts from red seaweed *Gelidium aserosa*. Int J Chem Res. 2011 Jan 1;2(20):27-9.
15. Ashwini S, Suresh BV, Saritha SM, Shantaram MS. Seaweed extracts exhibit anticancer activity against HeLa cell lines. Int J Curr Pharm Res. 2016 Dec 5;9(1):114-7. doi: 10.22159/ijcpr.2017v9i1.16632
16. Gupta P, Sinha D, Bandopadhyay R. Solation and screening of marine microalgae *Chlorella* sp. _pr1 for anticancer activity. Int J Pharm Pharm Sci. 2014 Oct 5;6(10):517-9.
17. Ravilla L, Lavanya M, Padmini R. Sustained anticancer effect by naringin-loaded zinc oxide nanoparticles in human lung adenocarcinoma A549 cells. Int J App Pharm. 2023;15:315-25. doi: 10.22159/ijap.2023v15i6.48848
18. Meerloo JV, Kaspers GJ, Cloos J. Cell sensitivity assays: The MTT assay. Methods Mol Biol. 2011 Mar 24;731:237-45. doi: 10.1007/978-

1-61779-080-5_20, PMID 21516412

19. Abdullah N, Patil AB. Designing of novel topical in situ polymeric film-forming solution spray formulation of antifungal Agent: *In vitro* activity and *in vivo* characterization. Int J App Pharm. 2022 Nov 21;14(1):169-84. doi: 10.22159/ijap.2022v14i1.43581
20. Johnson-Arbor K, Dubey R. Doxorubicin. StatPearls; 2023. Available from: https://www.ncbi.nlm.nih.gov/books/NBK459232 [Last accessed on 2024 Aug 20].
21. Cavassin FB, Baú-Carneiro JL, Vilas-Boas RR, Queiroz-Telles F. Sixty years of amphotericin B: An overview of the main antifungal agent used to treat invasive fungal infections. Infect Dis Ther. 2021 Feb 1;10(1):115-47. doi: 10.1007/s40121-020-00382-7, PMID 33523419
22. Mohamed NZ, Shaaban L, Safan S, El-Sayed AS. Phytochemical and metabolic profiling of the different *Podocarpus* species in Egypt: Potential antimicrobial and antiproliferative activities. Heliyon. 2023 Sep 8;9(9):e20034. doi: 10.1016/j.heliyon.2023.e20034, PMID 37810029
23. Dhaouafi J, Nedjar N, Jridi M, Romdhani M, Balti R. Extraction of protein and bioactive compounds from Mediterranean red algae (*Sphaerococcus coronopifolius* and *Gelidium spinosum*) using various innovative pretreatment strategies. Foods. 2024 Apr 28;13(9):1362. doi: 10.3390/foods13091362, PMID 38731733
24. Cabrita MT, Vale C, Rauter AP. Halogenated compounds from marine algae. Mar Drugs. 2010 Aug 9;8(8):2301-17. doi: 10.3390/md8082301, PMID 20948909
25. Martínez-Sanz M, Gómez-Mascaraque LG, Ballester AR, Martínez-Abad A, Brodkorb A, López-Rubio A. Production of unpurified agar-based extracts from red seaweed *Gelidium sesquipedale* by means of simplified extraction protocols. Algal Res. 2019 Jan 15;38:101420. doi: 10.1016/j.algal.2019.101420
26. Provonchee RB. Camden, Me. Agarose purif method using glycol. US Patent 1991 Feb 5;4(990):611.
27. Jönsson M, Allahgholi L, Sardari RR, Hreggviðsson GO, Nordberg Karlsson EN. Extraction and modification of macroalgal polysaccharides for current and next-generation applications. Molecules. 2020 Feb 19;25(4):930. doi: 10.3390/molecules25040930, PMID 32093097
28. Rupert R, Rodrigues KF, Thien VY, Yong WT. Carrageenan from *Kappaphycus alvarezii* (*Rhodophyta, Solieriaceae*): Metabolism, structure, production, and application. Front Plant Sci. 2022 May 10;13:859635. doi: 10.3389/fpls.2022.859635, PMID 35620679
29. Morgan DM. Tetrazolium (MTT) assay for cellular viability and activity. Methods Mol Biol. 1998;79:199879:179-83. doi: 10.1385/0-89603-448-8:179, PMID 9463833
30. van Meerloo JV, Kaspers GJ, Cloos J. Cell sensitivity assays: The MTT assay. Methods Mol Biol. 2011 Mar 24;731:237-45. doi: 10.1007/978-1-61779-080-5_20, PMID 21516412
31. Christenson J, Korgenski E, Relich R. Laboratory diagnosis of infection due to bacteria, fungi, parasites, and Rickettsieae. In: Principles and Practice of Pediatric Infectious Diseases. 5th ed. Amsterdam: Elsevier; 2017 Jul 18. p. 1422-34. doi: 10.1016/B978-0-323-40181-4.00286-3
32. Approved Standard. CLSI Document MO7. CLSI Methods for Dilution Antimicrobial Susceptibility Tests for Bacteria that Grows Aerobically. 9th ed., Vol. A9. Wayne: Clinical and Laboratory Standards Institute; 2012. Available from: https://microbenotes.com/mcfarland-standards
33. MestReNova, Ver. 6.0.2-5475, Mestrelab Research SL; 2009. Available from: https://mestrelab.com
34. Trivedi TJ, Kumar A. Efficient extraction of agarose from red algae using ionic liquids. Green Sustain Chem. 2014;4(4):190-201. doi: 10.4236/gsc.2014.44025
35. Yang JS, Xie YJ, He W. Research progress on chemical modification of alginate: A review. Carbohydr Polym. 2011 Feb;84(1):33-9. doi: 10.1016/j.carbpol.2010.11.048
36. Abu Bakar MH, Azeman NH, Mobarak NN, Mokhtar MH, Bakar AA. Effect of active site modification towards performance enhancement in biopolymer κ-carrageenan derivatives. Polymers. 2020 Sep 8;12(9):2040. doi: 10.3390/polym12092040, PMID 32911662
37. Kolender AA, Matulewicz MC. Hydrogel-forming algae polysaccharides: From seaweed to biomedical applications. Carbohydr Res. 2004;339(9):1619-29. doi: 10.1016/j.carres.2004.03.029, PMID 15183736
38. Jiang YP, Guo XK, Tian XF. Synthesis and NMR structural analysis of O-succinyl derivative of low-molecular-weight κ-carrageenan. Carbohydr Polym. 2005 Sep 21;61(4):399-406. doi: 10.1016/j.carbpol.2005.05.016
39. Gupta P, Goel A, Singh KR, Meher MK, Gulati K, Poluri KM. Dissecting the anti-biofilm potency of kappa-carrageenan capped silver nanoparticles against *Candida* species. Int J Biol Macromol. 2021 Mar 1;172:30-40. doi: 10.1016/j.ijbiomac.2021.01.035, PMID 33440209